# CERTIFICATION OF APPROVAL

DESIGN DIRECT-CURRENT (DC) MOTOR USING MATLAB

By

Syahrul Ashikin Azmi

A project dissertation submitted to the

Electrical & Electronic Engineering Programme

Universiti Teknologi PETRONAS

In partial fulfillment of the requirement for the

Bachelor of Engineering (Hons)

(Electrical & Electronics Engineering)

Approved:
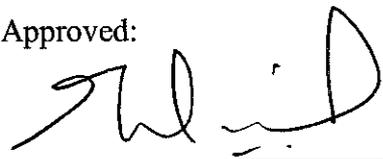
Mr. Nursyarizal Mohd. Nor

Project Supervisor

Nursyarizal Mohd Nor
Lecturer
Electrical Engineering Department
Universiti Teknologi PETRONAS
31750 Tronoh
Perak

UNIVERSITI TEKNOLOGI PETRONAS

TRONOH, PERAK

June 2004

CERTIFICATION OF ORIGINALITY

This is to certify that I am responsible for the work submitted in this project, that the original work is my own expect as specified in the references and acknowledgements, and that the original work contained herein have not been undertaken or done by unspecified sources or persons.
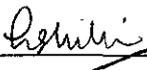
Syahrul Ashikin bt. Azmi

ABSTRACT

Electrical machine is a practical and dominant medium for achievement of productivity improvement. DC motor is defined when a machine reverses the conversion process to absorb energy in electrical form and reformat the energy to mechanical form on a sustained basis. As the field of industrial application of direct current is very wide, DC machine are produced both generators and motors, which suit for a large range of output powers, voltages, speeds and other. Therefore, an adequate design in dc motor is essential in order to meet the industrial practitioners' requirement. This study basically deals in designing dc motor based upon the customer specification using interactive computer software, MATLAB programming. The student is acted as the designer whom is requested by the customer to design a dc motor which produce correct simulation outcomes in order to meet the desired specifications. The project mainly concentrates on performing and formulating the required MATLAB programming added with C++ coding. The generated programs will demonstrate the plot-curves analysis of shunt excited dc motor design. An accurate dc motor design is reflected from the curves performed, whether it meet the performance specification or otherwise. MATLAB is fully utilized as the main tool to complete this area of study. As the initial stage of the study, iterative procedures have to be followed in designing the motor. The calculations for all parameters in each design stages need to be performed using the correct equations. The frame designation and units are referred to international standardization, which is NEMA MG-1 Standard. In order to enhance understanding of the conceptual design, literature review and theory is conducted concurrently with endeavor MATLAB programming. As continuous from preliminary stage, the study then focuses on application using MATLAB in order to perform the required analysis. Compared to previous design of dc motor, the NEMA frame designation and field winding arrangement play significant roles in differentiating the desired plot-curve representation.

ACKNOWLEDGEMENT

Firstly, I would like to express my gratitude to God, for His grace I was able to accomplish this project. I believe He has blessed me with sufficient strength and wisdom for me to carry out and complete this project.

My heartfelt thank goes to my supervisor, Mr, Nursyarizal Mohd. Nor for his continuous guidance and outstanding support that lead to the accomplishment of this project. Under his supervision, I was able to learn many new things especially on the subject regarding my project. I am very much indebted to him for the resources and precious time that he had provided me throughout the year. Truly, his generous guidance and help has put a light on my path in carrying out the project. Your sharing of knowledge, kindness and patience will always be appreciated.

My sincere thanks to Mr. Hussin Ibrahim of UTP Information Resource Center for his willingness to help me in finding materials regarding my project despite of his busy schedule. Special thanks to Mr. Yassin of UTP Power System Lab for his cooperation and teaching me about the construction of DC machine and also for sharing his information on the project topic.

I wish to thank my best friend Nukman Hussain, my roommates Suraya Hanim Abdullah Sani, my family, my housemates and my classmates who showed their concern and willingness to help for the success of my project from the beginning until the end. Your prayers, words of wisdom, encouragement and support have helped me through times where the path seemed to lead to a dead end. From deep inside my heart, thank you.

I would like to thank individuals such as the lab technicians, other lecturers and students whose names are not mentioned but involved directly or indirectly in the success of my project.

TABLE OF CONTENTS

LIST OF FIGURES

LIST OF SYMBOLS

τ_d	Developed Torque
K	e.m.f constant or torque constant
Φ_p	Total magnetic flux flowing from a field pole to armature core
I_a	Armature current
H	Magnetic field intensity produced by the current I_{net}
dL	Differential element of length along the path of integration
l_c	Mean path length of the core
μ	Magnetic permeability of material
B	Resulting magnetic flux density produced
dA	Differential unit of area
A	Cross-sectional area of the core
V_t	Rated Terminal Voltage
h_{pR}	Rated Output Power
n_{mR}	Speed at rated load
η_R	Goal Design Efficiency
n_m	Maximum speed at rated load
f	Frequency
p	Number of poles
τ_{dR}	Developed rated torque
d	Armature diameter
a	Armature stack length
D_f	Outside frame diameter
t_f	Frame thickness
v_T	Normalized sizing value.
N	Number of armature slots
n_c	Number of multiple per slot.
Z	Total conductors for the armature winding
k_E	Voltage constant
k_T	Torque constant

a	Number of lap winding
I_{aR}	Rated condition current
Φ_{pR}	Rated condition flux per pole
s_a	Stator conductor cross-section area
$_a$	Typical value of allowable stator current density for air-cooled machine
b_s	Armature slot width
w_c	Armature conductor with bare copper width
d_s	Slot depth
s_e	Gap between each adjacent coil
b_e	Armature coil depth at lower end-turn
g_e	Armature coil depth at upper end-turn
d_e	Width of each coil
λ_c	Gap between coil at lower end-turn
τ_c	Armature coil span for each turn
α	Angle of end-turn overhang
OH	Complete end-turn overhang
MLT_a	Mean length turn of an armature coil
R_a	Armature Resistance
ρ	Copper resistivity
T	Estimated average conductor temperature
B_{tra}	Apparent flux density at the tooth root
w_{tr}	Width of armature tooth
SF	Stacking factor
ψ	Pole arc-to-pole pitch ratio
τ_p	Number of armature slots spanned by the pole arc
m	An integer (1,2,3,.....)
λ	Armature slot pitch
K_c	Number of commutator bars
d_c	Commutator brush surface diameter
t_b	Brush dimension
w_b	Width of a single brush

b	Brush current density for rated load
n_b	Number of brushes per set
δ	Air gap length
δ_e	Effective length of the air gap
LF	Leakage factor.
B_f	Field flux density
A_f	Cross-sectional area of frame perpendicular to flux flow
w_f	Armature coil overhang
t_f	Frame thickness
h_p	Height of field pole
sk	Pole shank of field pole shape
sh	Pole shoe length of field pole shape
w_{sk}	Width of pole shank
B_a	Apparent tooth flux density at tooth ferromagnetic material
k_t	Permeability of the parallel air path
λ_3	Slot pitch at one-third the tooth depth
w_{t3}	Tooth width at one-third the tooth depth
mmf_p	Magnetomotive per pole
MLT_f	Mean length turn of the field winding
R_{fp}	Field resistance per pole
R_f	Field resistance of a series connection
I_f	Field current
N_f	Number of field turns
τ_{FW}	Friction and windage torque
ω_m	Motor Speed
P_{FW}	Mechanical rotational losses
E_a	Internal generated voltage
τ_{ind}	Induced Torque
P_{in}	Input Power
P_{out}	Output Power

CHAPTER 1

INTRODUCTION

1.1   Background of study

The electric machine age can be traced to 1831 with the invention by Michael Faraday of the disk machine-a true dc machine. Electric machines remained largely a laboratory and demonstration curiosity until the 1870s when Thomas Edison began commercial development of the dc generator to support house electrical power distribution. A major milestone in the history of electric machine was the patent of the three-phase induction motor by Nikola Tesla in 1888. Practical electric machines are bilateral energy converters that use an intermediary magnetic field link. When a machine reverses the conversion process to absorb energy in electrical form and reformat the energy to mechanical form on a sustained basis, it is called a motor.

DC machines can be thought of as a dying breed, but death will come slowly. Prior to the development of reliable, high-power solid-state switching devices, the dc motor was the dominant electric machine for all variable-speed motor drive applications. Even though "power electronic revolution" has led a significant shift from dc motor to adjustable-speed induction motor, this scenario not in possession of the facts that dc motor still become a machine of choice. Electric motors exist to convert electrical energy into mechanical energy. This is done by two interacting magnetic fields -- one stationary, and another attached to a part that can move. DC motors have the potential for very high torque capabilities (although this is generally a function of the physical size of the motor), are easy to miniaturize, and can be "throttled" via adjusting their supply voltage. DC motors are also not only the simplest, but the oldest electric motors. Due to the wide spear application of dc motor, it is crucial to comprehend the construction and underlying basis of the machine. Thus, designing dc motor is an eminent stage to allow concise presentation of basic processes and procedures underlying.

1

The designing process comprehends MATLAB programming as an essential tool in developing the design based on specification given. MATLAB is an integrated technical computing environment with combinations of numeric computation, advanced graphics and visualization, and a high-level programming. This software handles tedious calculation arising in electrical machine analysis. As a consequence, more exact dc motor design can be retained for analysis rather than the approximate design commonly introduced for the sake of computational simplicity. The MATLAB software will be programmed to generate outcomes result-plot in speed-torque, speed-line current, speed-output power and speed-efficiency curves of dc motor design to allow assessment with regard to performance specification. In preliminary stage, a literature review of the project is conducted as the initial cornerstone or underlying concept for development of dc machine. Subsequently, this study concentrates in performing calculations for each stage of design. A good understanding of the relationship and characteristic of the applied equations has to be achieved throughout the project. All the design procedures have to follow a standard guideline which is National Electrical & Manufacturer Association (NEMA) Standard MG-1. These guidelines can be organized into nameplate, environment and mechanical subdivisions. NEMA frame designations standardize envelopes and mounting dimensions, assuring interchangeability of motor. After completing all those phases, MATLAB programs are formulated to produce plot-curves analysis by associating all the parameters in each dc motor design phase.

1.2   Problem statement

DC machine turns out to be the most economical choice in the automotive industry for cranking motors, windshield wiper motors, blower motors and power window motors. DC machines already installed in areas where they are not presently the choice for new installations, yet still have many years of service life remaining. Thus, study on dc machine design is in order for enhancing acquaintance in the technical field. Besides of that, due to it's widely application in the industry, lots of demand on purchasing the machine still on-going. Therefore, in this project, a good invent of dc motor is needed to be performed and significantly has to fulfill industrial practitioners' requirement. The

student act as the developer or designer to design dc motor based on the performance specifications which are given by the customer or user. In addition, the design of the motor must meet international standardization, NEMA MG-1 and IEEE standards. The outcome of the design will be interpreted using MATLAB programming. MATLAB is a tool to ease the analysis intensity without a sacrifice in accuracy. The significant of the project is to ease to user to view and make analysis using MATLAB based upon the specifications that being given to the developer. Besides, it also provides an adequate reference for future developers in designing and makes comparison, as well as enhances improvement of the current design.

1.3   Objectives and Scope of Study

The objectives of this project are:

1. To study on basic processes and procedures underlying in designing a dc machine.

2. To perform required calculations for each design stages for MATLAB data input.

3. To design a dc motor that meets the specifications given and also follows national standardization (NEMA Standard MG-1) frame designation.

4. To generate programming or coding that engenders the required dc motor analysis using MATLAB software.

5. To simulate plot-curves result of the design to allow assessment with regard to the performance specifications.

The scope of this project is to study on the procedures required to design a dc motor. A logic flowchart is illustrated in Figure 3.1 as a basic guideline is used throughout the designing process. The procedures include volume and bore sizing, armature design, field pole design, magnetic circuit analysis, field winding design and finally performance analysis. Each design stages have its parameters that have to be understood and calculated. All calculations accomplished in each stage is included and tested in computer aided tool, namely MATLAB. The comparison between the manual and MATLAB calculations are compared respectively to check error if any. There are some

3

assumptions need to be considered in conjunction with result a good design practice. Besides, general understanding on standardization of overall design and also on the specific components in constructing dc motor is essential to make the design successful. The major part in this project is to formulate MATLAB programs to generate the correct plot-curves which suit the performance specifications. If the result does not meet the desired performance, the design then must be iterated by doing modification in the previous design stages.

Due to MATLAB application, therefore familiarization and learning process on MATLAB are done concurrently with the literature review of dc motor. Trial and error method also used in generating the coding if there is error happened. The MATLAB program will plot the speed-efficiency, the speed-torque, the speed-current and magnetization curves for the motor design to allow assessment based on the performance specification given by the user. Thus, MATLAB program with addition of C++ language has to be generated successfully to produce the outcome stated above. Furthermore, the project has become feasible to be carried out in the scope and timeframe given.

In addition, in accomplishing this project, problems such as absence or inadequacy of equipment or tools is barely possible as the project focuses mainly on design study and programming using MATLAB, in which the software is readily available.

CHAPTER 2

LITERATURE REVIEW AND THEORY

2.1 Construction of DC Motor

The stator of the DC motor has poles, which are excited by DC current to produce magnetic fields. The rotor has a ring-shaped laminated iron-core with slots. Coils with several turns are placed in the slots. The distance between the two legs of the coil is about 180 electric degrees. Figure 2.1 illustrates a typical dc motor construction that includes rotor, brush, stator with poles and field winding arrangement.
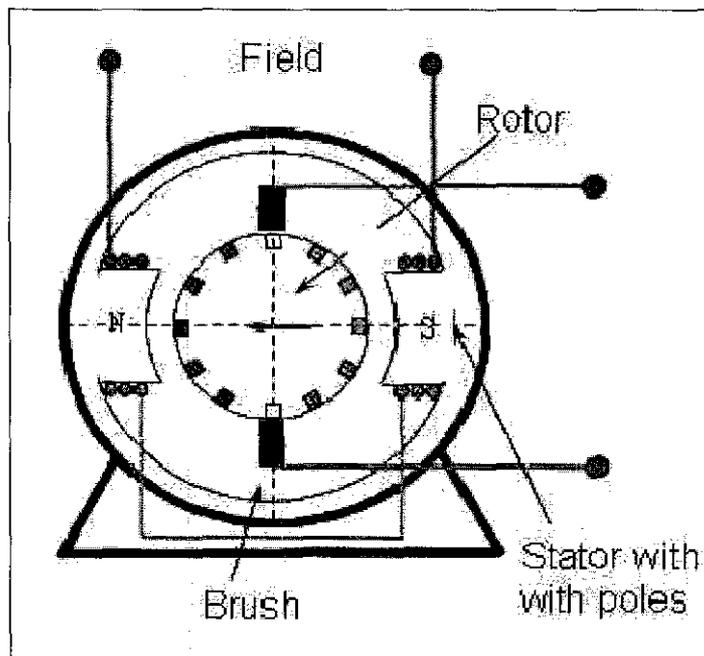
Figure 2.1: DC Motor Construction

The coils are connected in series. To keep the torque on a DC motor from reversing every time the coil moves through the plane perpendicular to the magnetic field, a split - ring device called a commutator is used to reverse the current at that point. The commutator illustrates in Figure 2.2 consists of insulated copper segments mounted in a cylinder. The electrical contacts to the rotating ring are called "brushes" since copper brush contacts were used in early motors. Modern motors normally use spring-loaded carbon contacts, but the historical name for the contacts has persisted. Two brushes are

5

pressed to the commutator to permit current flow. The brushes are placed in the neutral zone (magnetic field is close to zero) to reduce arcing.
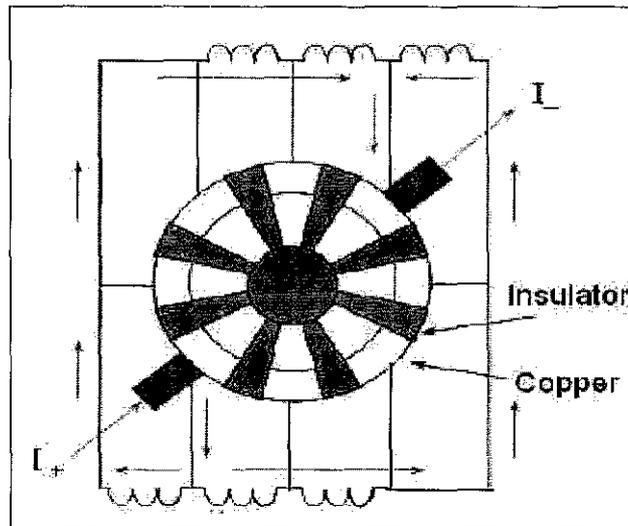
Figure 2.2: Concept of a Commutator

Figure 2.3 illustrates the stator of a large DC machine with several poles. The interpoles reduce the field in the neutral zone and eliminate arcing of the commutator. A compensation winding is placed on the main poles to increase field during high load. The iron core is supported by a cast iron frame.
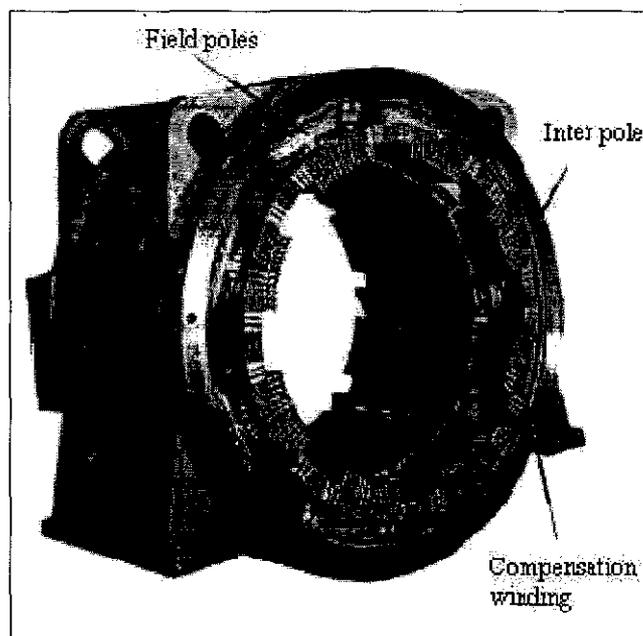
Figure 2.3: DC Motor Stator Construction

The following Figure 2.4 illustrates the rotor of a DC machine. The rotor iron core is mounted on the shaft. Coils are placed in the slots. The ends of the coils are bent and tied together to assure mechanical strength. The commutator mounted on the shaft consists of several copper segments, separated by insulation.
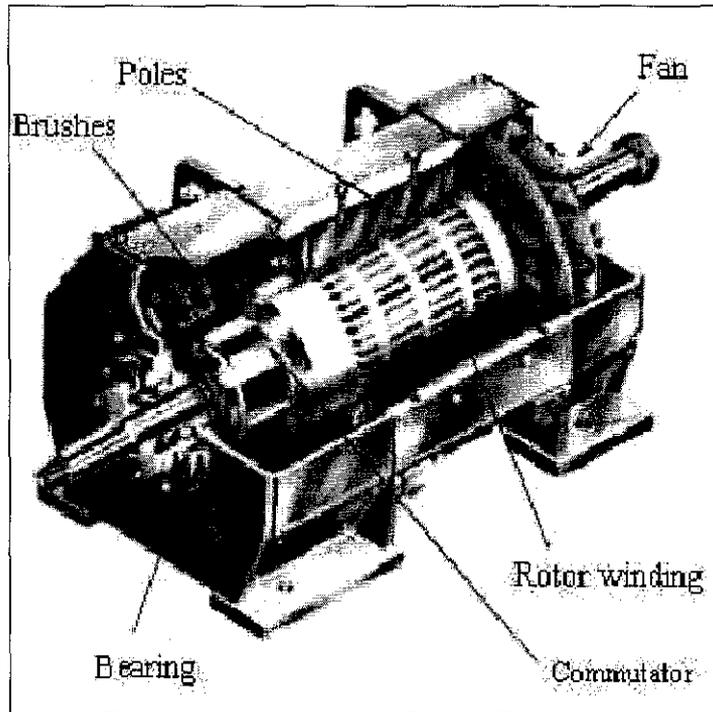
Figure 2.4: DC Motor Rotor Construction

Figure 2.5 illustrates the commutator of a large DC machine. The segments are made out of copper and mica insulation and placed between the segments. The end of each segment has a flag attached. The coil endings are welded to these flags. An insulated ring is placed on the coil ends to assure proper mechanical strength.
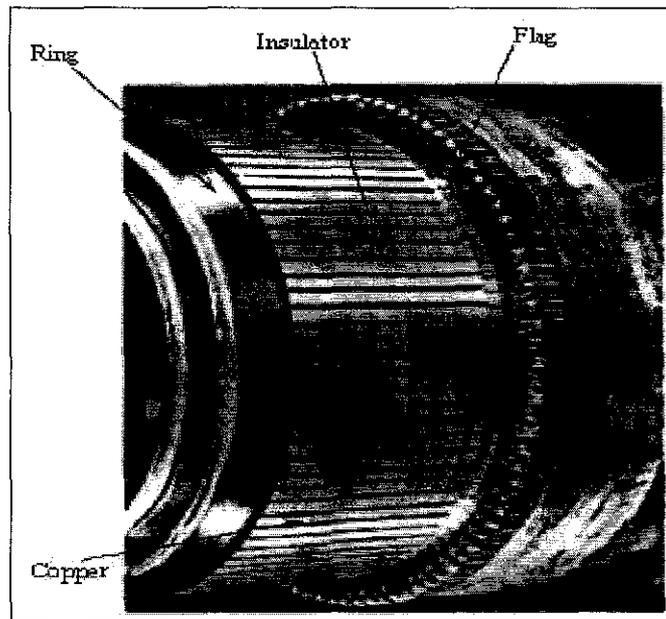
Figure 2.5: Commutator of a Large DC Motor

A DC motor is rarely installed in a situation where it is required to run at constant speed under constant load, since an AC induction motor performs such duties satisfactorily, costs only a fraction of the price of a DC machine of equal power and speed and requires minimal maintenance.

Many simple variable-speed systems are inherently stable in operation, so that the steady-state behaviour of a DC motor is frequently all that an engineer needs to take into consideration. For simple systems, a DC shunt motor excited from a single source is often satisfactory and provides a reasonable range of adjustable speed and torque. [1]

2.2   Torque

Magnetic lines of force flow in a direction of north to south between the poles of the stationery magnet. When magnetic lines of flux flow in the same direction, they repel each other. When they flow in opposite directions, they attract each other. The magnetic lines of flux around the conductors cause the loop to be pushed the direction shown by the arrows. This pushing or turning force is called torque and is created by the magnetic field of the pole pieces and magnetic field of the loop or armature.

Two factors determine the amount of torque produced by a direct current motor:

1. Total magnetic flux flowing from a field pole to armature core
2. Armature current of the respective pieces

The developed torque, τ_d, is represented in a given formula:

$$\tau_d = K\Phi_p I_a \dots\dots\dots\dots\dots\dots\dots\dots\dots\dots\dots\dots\dots\dots\dots (2.1)$$

Where:

K e.m.f constant or torque constant

Φ_p Total magnetic flux flowing from a field pole to armature core

I_a Armature current

One characteristic of a direct current motor is that it can develop torque at 0 rpm. [2]

2.3 Torque, voltage and current relationship of motor operation

If a load is connected to the motor, it must furnish more torque to operate the load. This causes the motor to slow down. When the motor speed decreases, the rotating magnetic field cuts the rotor bars at a faster rate. This causes more voltage to be induced in the rotor and therefore, gained more current. The increased current flow produces a stronger magnetic field in the rotor, which causes more torque to be produced. The increased current flow in the rotor also causes an increased current flow in the stator. This is why motor current will increase as load is added. [2]

2.4 Production of magnetic field

The basic law governing the production of a magnetic field by a current is Ampere's Law:

$$\int H . dL = I_{net} \dots\dots\dots\dots\dots\dots\dots\dots\dots\dots\dots\dots\dots\dots\dots (2.2)$$

Where:

H Magnetic field intensity produced by the current I_{net}

dL Differential element of length along the path of integration

In SI units, I and H are measured in ampere and ampere-turns per meter respectively. Figure 2.6 shows a rectangular core with a winding of N turns of wire wrapped about one leg of the core. If the core is composed of iron or other similar metals, essentially all magnetic field produced by the current will remain inside the core, so the path of integration in Ampere's Law is the mean path length of the core l_c. The current passing within the path of I_{net} is Ni, since the coil of wire cuts the path of integration N times while carrying current i. Thus, the law becomes:

$$Hl_c = Ni \dotfill (2.3)$$

$$H = \frac{Ni}{l_c} \dotfill (2.4)$$
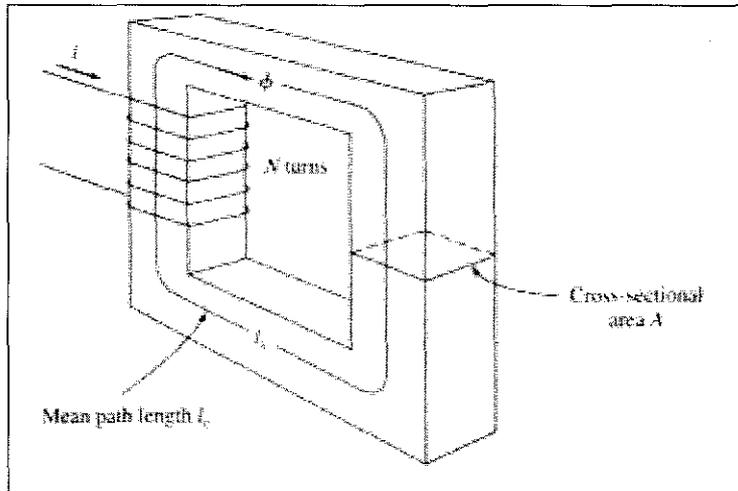
Figure 2.6: Magnetic Core

The magnetic field intensity H is in sense a measure of the effort that a current is putting into the establishment of a magnetic field. The strength of magnetic flux produced in the core also depends on the material of the core which typically ferromagnetic material. The relationship between H-field and the resulting magnetic flux density, B produced within a material is given by:

$$B = \mu H \dotfill (2.5)$$

Where:

H Magnetic field intensity

μ Magnetic permeability of material

B Resulting magnetic flux density produced

By combination of equation (2.4) and (2.5), the magnetic of flux density, B, is given by:

$$B = \mu H = \frac{\mu N i}{l_c} \dots\dots\dots\dots\dots\dots\dots\dots\dots\dots\dots\dots\dots (2.6)$$

The total flux in a given area is indicated by:

$$\phi = \int_A B.dA \dots\dots\dots\dots\dots\dots\dots\dots\dots\dots\dots\dots (2.7)$$

Where:

dA Differential unit of area

If the flux density vector is perpendicular to a plane of area A, and if flux density is constant throughout the area, then this equation reduces to:

$$\phi = BA \dots\dots\dots\dots\dots\dots\dots\dots\dots\dots\dots\dots\dots (2.8)$$

Thus, the total flux in the core due to the current in Figure 2.1 due to the current, i, in the winding is given by:

$$\phi = BA = \frac{\mu N i A}{l_c} \dots\dots\dots\dots\dots\dots\dots\dots\dots\dots\dots (2.9)$$

Where:

A Cross-sectional area of the core.

l_c Mean path length of the core.   [3]

2.5   Magnetic Behaviour of Ferromagnetic Materials

The magnetic permeability was defined by equation (2.5) explained that the permeability of ferromagnetic materials is very high, up to 6000 times the permeability of free space. The behaviour of magnetic permeability in a ferromagnetic material is illustrated by applying a direct current to the core shown in Figure 2.6. The current

11

started with 0 A and slowly working up to the maximum permissible current. When the flux produced in the core is plotted versus the magnetomotive force producing it, the resulting plot looks like Figure 2.7a. This type of plot is called a saturation curve or a magnetization curve. At first, a small increase in the magnetization force produces a huge increase in the resulting flux. After a certain point, though, further increases in the magnetomotive force produce relatively smaller increases in the flux. Finally, an increase in the magnetomotive force produces almost no change at all. The region of Figure 2.7a in which the curve flattens out is called the saturation region, and the core is said to be saturated. In contrast, the region where the flux changes very rapidly is called the unsaturated region of the curve, and the core is said to be unsaturated. The transition region between unsaturated and saturated region is often called the knee of the curve. On the other hand, Figure 2.7b illustrates a plot of magnetic flux density B versus magnetizing intensity H. From the plot, it is clearly visualize that magnetizing intensity is directly proportional to magnetomotive force and magnetic flux density is directly proportional to flux for any given core. Therefore, the relationship between B and H has the same shape as the relationship between flux and magnetomotive force. Figure 2.8 illustrates a magnetization curve for a typical piece of steel which plotted more detail and with magnetizing intensity on a logarithmic scale.

The advantage of using a ferromagnetic material for cores in electric machines is that it gain more flux for a given magnetomotive force with iron compared to air. Since real motors and generators depend on magnetic flux to produce voltage and torque, they are designed to produce as much as flux as possible. As a result, most machines operate near the knee of magnetization curve and the flux in their cores is not linearly related to the magnetomotive force producing it. [3]

12
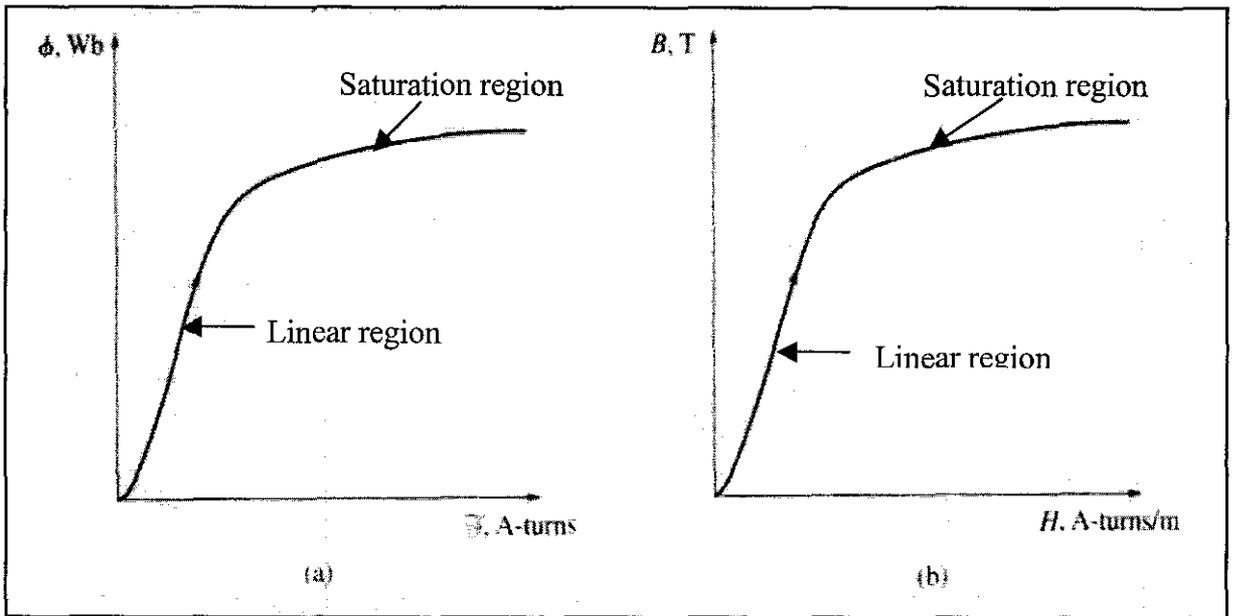
Figure 2.7a: DC Magnetization Curve for Ferromagnetic Core

Figure 2.7b: Magnetization Curve of Flux Density versus Magnetizing Intensity
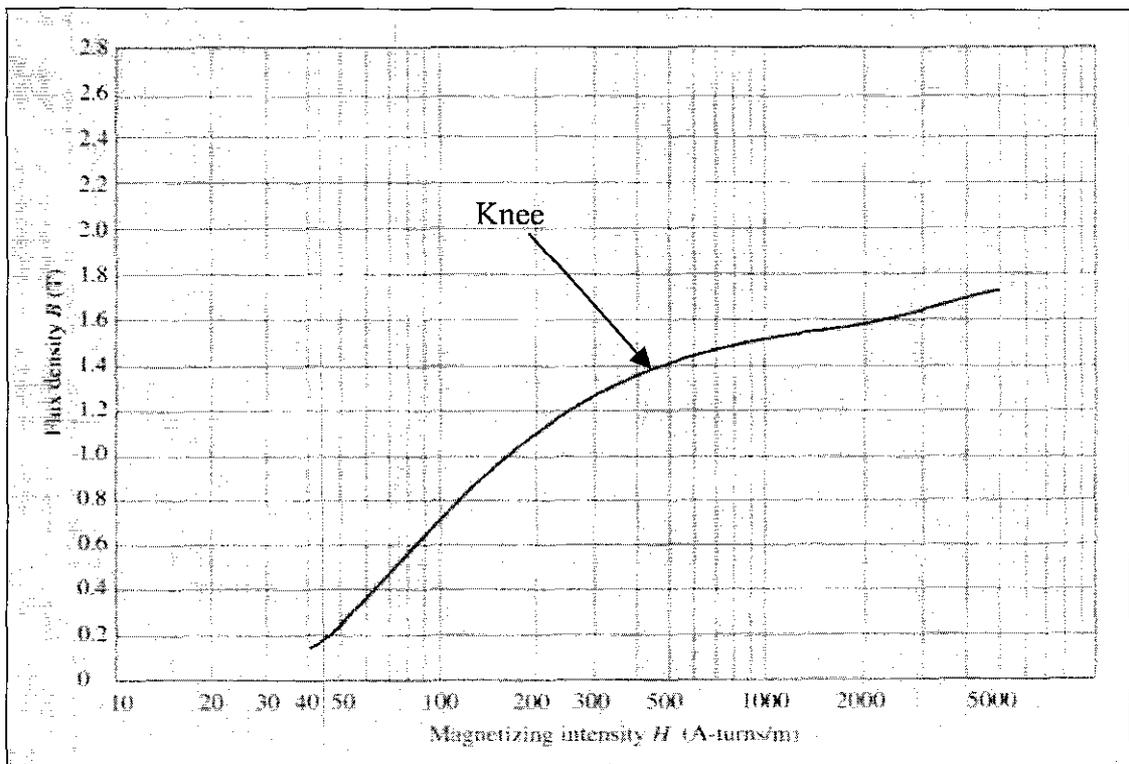
Figure 2.8: Magnetization curve a typical piece of steel

13

CHAPTER 3

METHODOLOGY / PROJECT WORK

3.1 Research Study

To accomplish this project, it has to begin with information gathering activity. The resources for this research include books, journals, articles, reports and the internet.

3.1.2 Research on DC Motor Design Theory

This method is the essential part for the project as it implies lots of courage and effort to gain well-understanding and familiarization of the topic proposed. A study has being performed, in order to understand the underlying basis and also the equations in designing dc machine. This study also includes on the theoretical part of dc motor and also identifies all the parameters needed in each design phase.

3.2 Perform calculations of all parameters for every design stages

After all the parameters required being identified, calculations have been performed. The formulas of all calculated parameters were found from the books and paper work. To ensure the accuracy of the calculation, MATLAB program is formulated for comparison. The parameters of each stage are used as data input for MATLAB programming.

3.3 Discussion with supervisor

This approach act is the crucial part for the project progress. With the assistance of the supervisor, all the finding and the problem face could be discuss and being evaluate together in order to achieve the solution. The discussion also provides the platform for the idea brainstorming, which help on the progress made on the project.

3.4 Implementation (MATLAB programming)

Since the project mainly involve programming using MATLAB software, therefore the familiarization stage is beneficial in order to implement the coding design of the project. This method is essential and important in order to produce the desired result. The

software is a tool to ensure that the design platform accommodate with the specification given by the supervisor. Furthermore, several trial programming are beneficial to be performed for preliminary understanding on the project. Trial-and-error also one of alternative that will be accommodate whenever there is any error occurred in the program. However, this alternative is based on knowledge and discussion with supervisor and who are expert in the field of study. The programs basically formulated by extracted some of the parameters in the design process to generate the specific outcome. Different outcome might need different data to be accommodated within it.

As a clearer view of procedure identification of the project, a graphical logic flowchart and brief descriptions of each phase is stated in Figure 3.1.
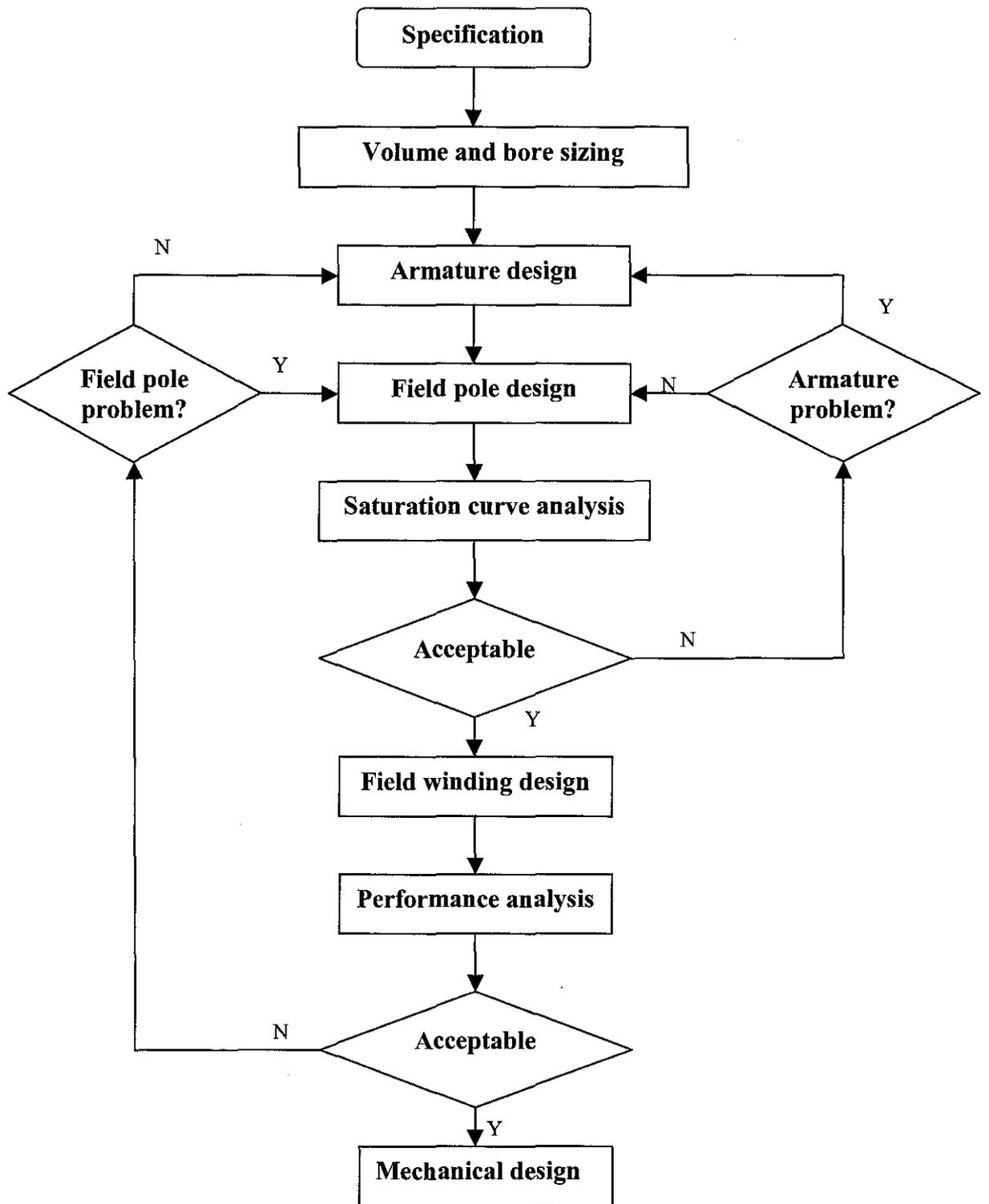
Figure 3.1: Logic flowchart of dc motor design

3.5 Description of each dc motor design stages

3.5.1 1st stage: Specification

1. The specification is given the customer and for frame designation of the design must followed NEMA MG-1 standard.

3.5.2 2nd stage: Volume and Bore Sizing

1. The initial sizing process of dc motor design is to set the outside frame diameter (D_f) which in this project NEMA frame designation, $D_f = P$.

2. The design procedure starts with three important parameters namely armature diameter, rated developed torque and armature stack length.

3.5.3 3rd stage: Armature design

1. In this stage, some calculations have to be performed such as calculate the number of armature slots, voltage and torque constants, rated current and flux per pole and slot design.

2. These calculations are essential in order to proceed to the next stage.

3.5.4 4th stage: Field pole design

1. To design of actual field pole, two items must be addressed which are air gap length and frame thickness.

2. Based on the satisfied result, the reluctance of magnetic circuit around flux path remains nearly constant regardless of armature position.

3.5.5 5th stage: Saturation curve analysis

1. This stage is the major role in the design process where all the data correlate in above stages are formulated in Matlab program to produce magnetization curve of dc motor. An analysis of the design begins at this point.

2. The open-circuit saturation curve (Φ_p vs mmf_p) must be determined prior to the analysis. The field winding cannot be designed for the rated point of operation until the mmf requirement is satisfied. Using Matlab, magnetization curve and B-H curve have to be performed.

17

3.5.6 6th stage: Field winding design

1. The field winding arrangement is designed to fit into the available space surrounding field pole physically. In the project, the field winding arrangement is shunt excited dc motor.

2. A layout drawing of field pole and frame is necessary to determine space availability.

3.5.7 7th stage: Performance analysis

1. At this stage, all the calculation involved in the previous stages also are formulated in MATLAB software. The analysis continued with performance analysis of the design whether meet the performance requirement or otherwise.

2. The expected outcomes are plot-curves of speed-torque, speed-line current, speed-output power and speed-efficiency of shunt dc motor. All these curves have to be understandable and analyze their characteristic with respect to the selected field winding arrangement.

3. The MATLAB program is formulated by modification of the required design to read OCC (open-circuit circuit) that has been saved by the last run of the program. The simulation of the result will predicted the performance of designed motor whether suit the specification or otherwise.

3.5.8 8th stage: Mechanical classification

1. Basically in this stage, the prototype of the motor will be made with associated by mechanical department.

2. The design of DC motor is successfully completed.

3.6   Tool required

3.6.1   MATLAB software

The main and only tool that is required for this project is MATLAB software. For the project, MATLAB version 6.5 is being used. MATLAB is a robust simulation which utilizes mathematical equations to generate the outcome. In order to achieve the objectives of the project, pure programming is used instead of simulation. This required basic knowledge and exposure on the software application.

CHAPTER 4

RESULT AND DISCUSSION

4.1   Specification

Specification is the first constituent encountered in the flow chart illustrated in methodology. The outcome of designing processes is considered success if it can meet the specification given. The specification for dc motor design is stated as below.

1. Rated Terminal Voltage, V_t = 415 V.
2. Rated Output Power, h_{pR} = 400 hp.
3. Speed at rated load, n_{mR} = 1 800 rpm.
4. Goal Design Efficiency, η_R = 95%.
5. Maximum speed at rated load, n_{max} = 3 000 rpm.
6. NEMA Frame designation   = 583-AT.
7. Frequency, f = 50 Hz.
8. Number of pole, p = 4.

A standard of the National Electrical Manufacturers Association (NEMA) defines a product, process, or procedure with reference to one or more of the following:

1. Nomenclature.
2. Composition.
3. Construction.
4. Dimensions.
5. Tolerances.
6. Safety.
7. Operating characteristics.
8. Performance.
9. Ratings.
10. Testing.
11. The service for which it is designed.

The standards play a vital part in the design, production, and distribution of products destined for both national and international commerce. Sound technical standards benefit the user, as well as the manufacturer, by improving safety, bringing about economies in product, eliminating misunderstandings between manufacturer and purchaser, and assisting the purchaser in selecting and obtaining the proper product for his particular need. The basic NEMA frame dimensions is illustrated in Appendix I. Specific dimension values for a selected group of frames that being used in dc motors over range from 5 to 800-hp motors are also found in Appendix A. For this project, 583 AT frame designation are selected.

4.2   1st stage: Volume and Bore Sizing

The design procedure starts with Volume and Bore Sizing. In this stage, there are three important elements that must be accomplished in order to complete this stage, namely:

1. Developed rated torque (τ_{dR})
2. Armature diameter (d)
3. Armature stack length (ℓ_a)

4.2.1   Developed rated torque (τ_{dR})

The rated output power and full-load speed are used to calculate rated condition shaft torque or full-load torque, τ_{dR}, for a dc motor, given in equation (4.1):

$$\tau_{dR} = \frac{5250 hp_R}{n_{mR}} \quad ft.lbs \quad \text{..............................} (4.1)$$

Where:

h_{pR} Rated output power (unit in hp)

n_{mR} Speed at rated load (unit in rpm)

The rated developed torque is under reasonable assumption of 5 percent rotational losses. This torque is required to keep the load running continuously at a fixed speed.

From equation (4.1), the developed rated torque, τ_{dR} is:

$$\tau_{dR} = \frac{5250 \times 400}{0.95 \times 1800} \; ft.lbs$$

$\tau_{dR} = 1\,228.07\,ft\text{-}lb$

4.2.2 Armature diameter (*d*)

In sizing process of dc motor design, one of the important parameter is to set the outside frame diameter (D_f). Thus, by referring to NEMA frame designation (583AT) which D_f is equal to *P*, in the respective table illustrated in Appendix A. Usually, adequate frame thickness (t_f) and radial depth to accommodate field pole design results if the armature diameter is taken to be in range of:

$$0.55 D_f \le d \le 0.65 D_f \dots\dots\dots\dots\dots\dots\dots (4.2)$$

From the table, the frame designation being used is 583AT frame where $D_f = P = 29.00$ inch. Using mean value of equation (4.2),

$$0.55(29.00) \le d \le 0.65(29.00)$$

$$15.95 \le d \le 18.85$$

$$d = 0.6 D_f = 0.6\,(29.00) = 17.4\,in$$

4.2.3 Armature stack length (l_a)

In order to minimize sizing value, the values of current density and flux density are maintained at the limit allowed by the ability to cool armature conductors and by saturation limits imposed in ferromagnetic material. Therefore, the formula to calculate armature stack length, l_a:

$$\frac{d^2 l_a}{\tau_{dR}} = constant = v_T \dots\dots\dots\dots\dots\dots\dots (4.3)$$

Where:

v_T Normalized sizing value.

d   Outside frame diameter (unit in inch).

The sizing value v_T must be increased as the machine size decreases to allow for acceptable tooth root flux density. The graph in Appendix B represents the values of v_T used for initial sizing of dc motor depending on the method of cooling. The graph is valid for rated speed of approximately 1800 rpm. The value of v_T is inversely proportional to the speed. Based on the graph, the approximate v_T is 1.91 $in^3/ft.Ib$.

$$d^2 l_a = v_T \tau_{dR} = 1.91 \times 1\,228.07 = 2\,345.6137\ in^3$$

Thus,

$$l_a = \frac{d^2 l_a}{d^2} \ \dots\dots\dots\dots\dots\dots\dots\dots\dots\dots\dots\dots\dots(4.4)$$

$$l_a = \frac{2\,345.6137}{17.4^2}$$

$$l_a = 7.7474\ in$$

4.3 Armature Design

Armature Design is the 2nd stage of designing dc machine. In this stage, certain parameters have to be calculated which are:

1. Number of armature slots.
2. Voltage and torque constant.
3. Rated current and flux per pole.
4. Slot design.
5. Coil characterization.
6. Flux density check.
7. Commutator design.

A flowchart for armature design also include in Appendix C for clearer view of the process.

4.3.1 Number of armature slots

In order to minimize flux pulsation along the pole face and produce a slot width that allows for good slot wedge integrity, the armature slot pitch (λ) should typically be in the range:

$$1 \leq \lambda = \frac{\pi d}{N} \leq 1.5 \text{ inch} \dots\dots\dots\dots\dots\dots\dots\dots\dots (4.5)$$

Where:

d Outside frame diameter (unit in inch).

N Number of armature slots

For $d \leq 20$ inch, the lower end of the range usually results in better design.
If slot pitch $\lambda = 1$, the equation above gives:

$$N = \frac{\pi d}{\lambda}$$

$$= \frac{\pi \times 17.4}{1}$$

$$= 54.66 \text{ slots} \approx 54 \text{ slots}$$

Use N= 54 slots. With N chosen,

$$\lambda = \frac{\pi \times 17.4}{54}$$

$$= 1.0123 \text{ in}$$

Since the armature lamination stack experiences a reversing flux, the number field poles should be selected to give a cyclic frequency in the range of 45 to 70 Hz for operation at rated speed.

$$45 \leq \frac{p n_{mR}}{120} \leq 70 \text{ } Hz \dots\dots\dots\dots\dots\dots\dots\dots\dots (4.6)$$

Where:

p Number of poles.

n_{mR} Speed at rated load (unit in rpm).

From the specification, the design motor should be 4-pole machine, therefore the cyclic frequency is:

$$\frac{pn_{mR}}{120} = \frac{4 \times 1800}{120}$$

$$= 60 \text{ Hz}$$

This value is within the acceptable range for acceptable core losses. In addition, a good design practice is to select the number of armature slots (N) as an integer that falls in the range:

$$11.5p \le N \le 15.5p \quad \cdots\cdots\cdots\cdots\cdots\cdots\cdots\cdots\cdots\cdots (4.7)$$

$$\frac{N}{p} = \frac{55}{4} = 13.75$$

Thus, the value lies within the acceptable range for slots per pole.

4.3.2 Voltage and torque constant

In this design, the consideration is taken in a case where a simplex winding (a=p). Integral horse-power dc machine commonly has a single-turn armature coil with multiple coils per slot (n_c) with two or three coils per slot being typical values. The total conductors for the armature winding, Z, is given by:

$$Z = 2n_cN \quad \dots\dots\dots\dots\dots\dots\dots\dots (4.8)$$

Where:

n_c Number of multiple coils per slot.

       (3 coils per slot for design trial for 3-phase dc motor).

Thus, the total armature conductors are:

$$Z = 2 \times 3 \times 54 = 324 \text{ conductors}$$

The voltage and torque constants, k_E and k_T (unit in flux) are given by, respectively in equation (4.9) and (4.10):

$$k_E = \frac{pZ}{a60 \times 10^8} \quad \text{.................................... (4.9)}$$

Where:

a Number of lap winding (consider simplex winding, $a=p=4$)

$$k_E = \frac{4 \times 33}{4 \times 60 \times 10^8} = 5.5 \times 10^{-8} \text{ V/line.rpm}$$

$$k_T = \frac{pZ}{a8.525 \times 10^8} \quad \text{................................... (4.10)}$$

$$k_T = \frac{4 \times 330}{4 \times 8.525 \times 10^8} = 3.871 \times 10^{-8} \text{ ft} - \text{lb/line.A}$$

4.3.3 Rated current and flux per pole

The rated condition current, I_{aR}, is calculated using equation (4.11).

$$I_{aR} = \frac{746hp_R}{\eta_R V_t} \quad \text{................................. (4.11)}$$

Where:

η_R Design goal efficiency (unit in %).

V_t Rated Terminal Voltage (unit in Voltage).

$$I_{aR} = \frac{746 \times 400}{0.95 \times 415} = 756.88A$$

If reasonable value rotational losses are 5 % of the machine power rating, the rated condition flux per pole, Φ_{pR} is:

$$\Phi_{pR} = \frac{\tau_{sR} / 0.95}{k_T I_{aR}} \text{lines} \quad \text{............................. (4.12)}$$

26

$$\Phi_{pR} = \frac{1228.07}{3.871 \times 10^{-7} \times 756.88}$$
$$= 4.1915 \text{ Megalines}$$

4.3.4 Slot design

After rated armature current and rated flux per pole is established, the armature slot, tooth and coil can be seized as shown in Figure 4.1.
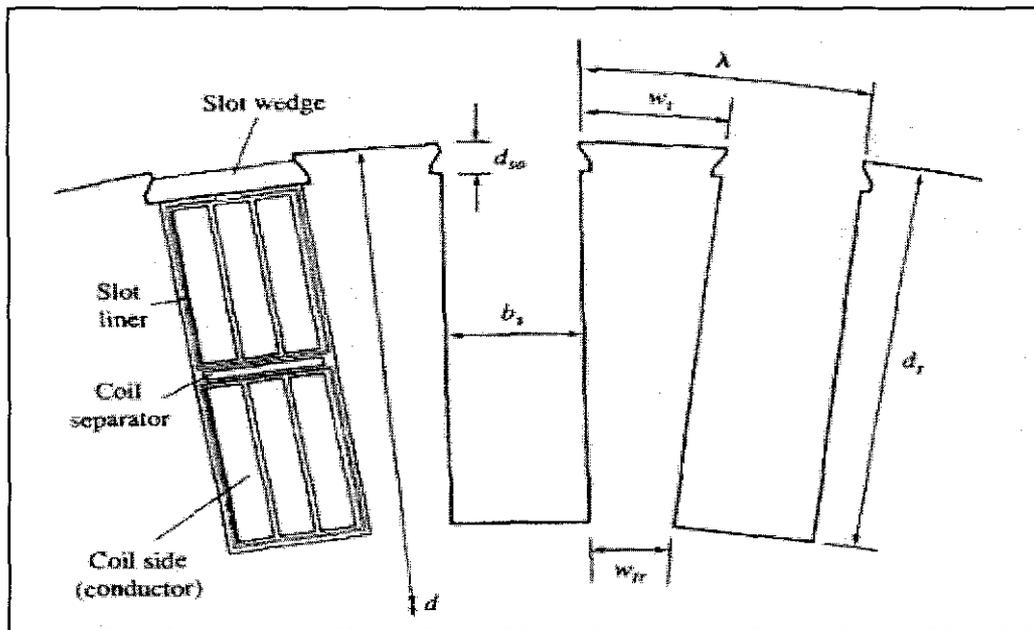
Figure 4.1: Armature slot section view

In dc machine design, it is rarely to find a standard square wire size compatible with the selected slot dimensions. However, magnet wire manufacturers readily supply rectangular conductors drawn to desired dimension and served with film insulation.

The value of stator conductor cross-section area, s_a, is given as follows:

$$s_a = \frac{I_{aR}}{a\Delta_a} \quad \dots\dots\dots\dots\dots\dots\dots\dots\dots\dots\dots\dots\dots\dots\dots\dots \text{(4.13)}$$

Where:

Δ_a Typical value of allowable stator current density for air-cooled machine.

The acceptable range for Δ_a is:

$$500 \le \Delta_a \le 800 \text{ A/cm}^2 \text{ or } 3200 \le \Delta_a \le 5200 \text{ A/in}^2$$

In this design, consideration has been made that the machine is a self-ventilated which will fall in the mid-range of $3200 \le \Delta_a \le 5200$ A/in^2. Let $\Delta_a = 4000$ A/in^2, thus the stator conductor area, s_a, is:

$$s_a = \frac{756.88}{4 \times 4000} = 0.0473 \text{ in}^2$$

For good design, the armature slot width, b_s is selected such that:

$$0.4\lambda \le b_s \le 0.5\lambda \text{ .... (4.14)}$$

In an attempt to have an armature slot width, b_s in the midrange of equation (4.14), an armature conductor with bare copper width, w_c, is selected equal to 0.110 inch. The armature conductor will be insulated with a high temperature film wrap to a thickness of 0.003 inch. Therefore, conductor height, h_c, is:

$$h_c = \frac{s_a}{w_c} \text{ .... (4.15)}$$

Where:

s_a Armature conductor area (unit in inch^2)

w_c Armature conductor with bare copper (unit in inch)

$$h_c = \frac{0.0473}{0.110} = 0.43 \text{ in}$$

The slot depth, d_s, on the other hand falls in the range of:

$$2b_s \le d_s \le 4b_s \text{ .... (4.16)}$$

In addition to containment of two coil sides, the slot must assure adequate insulation between coil sides and accept a means of retaining the coil sides (slot separator) and accept a means of retaining the coil sides (slot wedge) as illustrated in Figure 4.1.

Allowing for irregularity in material, d_s is chosen as 1.150 inch. The slot depth-to-width ratio is:

$$\frac{d_s}{b_s} = \frac{1.150}{0.450} = 2.55$$

From calculated slot depth-to-width ratio, d_s/b_s, it is found that the ratio falls within the range suggested by equation (4.16).

4.3.5 Coil characteristic

Coil is one or more turns of wire grouped together and mounted on the drum-wound armature in order to cut lines of flux. According to the degree of closure produced by winding, there are 2 types of armature winding:

1. Open coil winding is when winding does not close on itself and usually employed in ac machine.

2. Closed-coil winding is when winding which closes on itself. DC machine employ only this winding in order to provide for the commutation of the coils.

The winding may be lap windings or wave windings. As mention earlier, lap winding is used due to its capability in producing more parallel paths for large current application. In lap winding, the finish of each coil is connected to the start of next coil so that winding or commutator pitch is unity. In a simple lap winding, front and back pitches are always odd and differ by 2, while the average pitch is an even number. In a one turn winding, the total number of segments required is equal to one-half the number of armature conductors, since each commutator segment is connected to two conductors.

The end-turn layout of an armature coil is shown by Figure 4.2. The end-turn projection of armature coil is directly impacts the axial length of armature assembly, therefore it is desirable to hold the projection to as small a value as practically possible.

The design objective is usually accomplished if the following dimensions of Figure 4.2 are maintained:

1. Gap between each adjacent coil, $s_e = 0.125$ to 0.250 inch.

2. Armature coil depth at lower end-turn, $b_e = 0.50$ to 1.00 inch.

3. Armature coil depth at upper end-turn, $g_e = d_s$

4. Width of each coil, $d_e = s_e + b_s$

5. Gap between coil at lower end-turn, $\lambda_c = \dfrac{\pi(d - d_s)}{N}$

6. Armature coil span for each turn, $\tau_c = \text{integer} \dfrac{N}{p} \times \lambda_c$

7. Angle of end-turn overhang, $\alpha = \sin^{-1} \dfrac{d_e}{\lambda_c}$
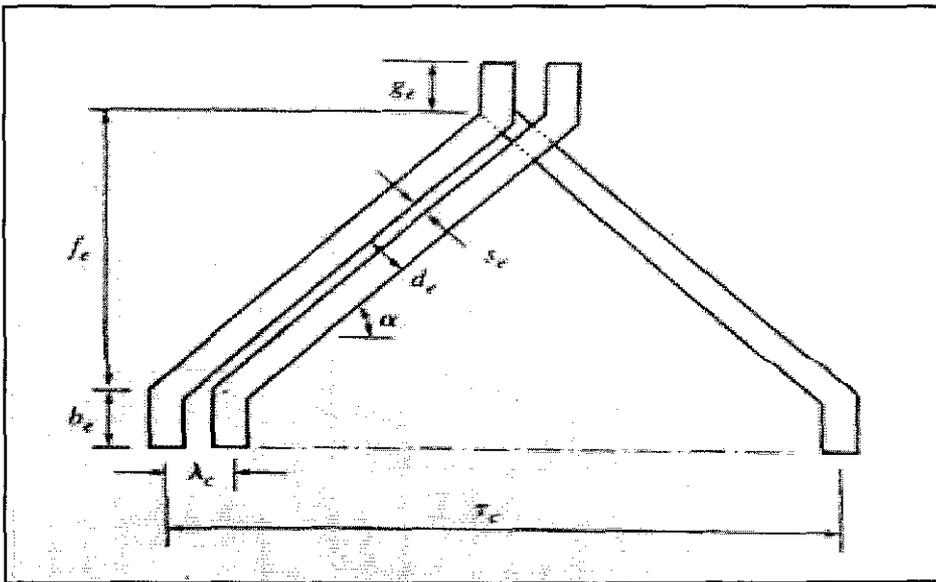
Figure 4.2: Armature coil end turn

Complete end-turn overhang, OH for each turn, is given by:

$$OH = b_e + \frac{\tau_c}{2} \tan\alpha + g_e \dots\dots\dots\dots\dots (4.17)$$

For the coil end-turn overhang (OH) calculation, let:

$$s_e = 0.125 \text{ inch.}$$

$$b_e = 0.50 \text{ inch.}$$

30

$$g_e = d_s = 1.150 \text{ inch.}$$

$$d_e = 0.125 + 0.45 = 0.575 \text{ inch.}$$

$$\lambda_c = \pi \frac{(17.4 - 1.15)}{54} = 0.9454 \text{ in}$$

$$\tau_c = \text{integer} \frac{54}{4} \times 0.9454 = 12.7629 \text{ in}$$

$$\alpha = \sin^{-1} \frac{0.575}{0.9454} = 37.46^\circ$$

Using all the parameters calculated above, the complete end-turn overhang, *OH* is calculated by equation (4.17):

$$OH = 0.50 + \frac{12.7629}{2} tan\,37.46^\circ + 1.15$$
$$= 6.5396 \; inch$$

The mean length turn (*MLT$_a$*) of an armature coil can be determined as:

$$MLT_a = 2 \left(\frac{\tau_c}{cos\,\alpha} + 2b_e + 2g_e + l_a \right) \dots\dots\dots\dots\dots (4.18)$$

$$MLT_a = 2 \left(\frac{12.7629}{cos\,37.46^\circ} + 1 + 2.3 + 7.7474 \right)$$

$$= 54.2521 \text{ inch}$$

Then, the value of resistance for armature circuit can be calculated using equation (4.19):

$$R_a = \rho \frac{MLT_a(Z/2)}{a^2 s_a} \dots\dots\dots\dots\dots\dots\dots (4.19)$$

Where:

ρ Copper resistivity (equivalent value is 0.69 x 10^{-6} Ω. inch at 20°C).

The value must be adjusted to the anticipated operating temperature (T) of armature winding by equation (4.20):

$$\rho = \frac{234.5 + T}{254.5}\left(0.69 \times 10^{-6}\right) \dots\dots\dots\dots\dots\dots\dots\dots(4.20)$$

$$\rho = \frac{234.5 + 150}{254.5}\left(0.69 \times 10^{-6}\right)$$

$$= 1.042 \times 10^{-6} \ \Omega.\text{inch}$$

Where:

T Estimated average conductor temperature, $T = 150°C$.

Therefore, the armature resistance, R_a, is calculated using equation (4.19):

$$R_a = 1.042 \times 10^{-6}\left(\frac{54.2521 \times 162}{4^2 \times 0.04505}\right)$$

$$= 0.0127 \ \Omega$$

4.3.6   Flux density check

Prior to begin the commutator design, critical flux density for armature tooth root should be checked. The apparent flux density at the tooth root, B_{tra}, of Figure 4.1 is given by:

$$B_{tra} = \frac{\Phi_{pR} \times p}{\psi \times N \times w_{tr} \times l_a \times SF} \dots\dots\dots\dots\dots\dots\dots\dots (4.21)$$

Where:

w_{tr} Width of armature tooth (unit in inch).

$$w_{tr} = \left[\frac{\pi(d - d_s)}{N}\right] - b_s$$

$$= \left[\frac{\pi(17.4 - 2.3)}{54}\right] - 0.45 \dots\dots\dots\dots\dots\dots (4.22)$$

$$= 0.4285 \text{ inch}$$

Φ_{pR} Rated flux per pole (unit in Megalines).

l_a Armature stack length (unit in inch).

SF Stacking factor.

p	Number of pole.
N	Number of turns.
ψ	Pole arc-to-pole pitch ratio.

The value of stacking factor (SF) is in range of $0.94 \le$ SF ≤ 0.97, and depends on the lamination thickness as well as the axial assembly pressure of the armature lamination stack. In this design, the value of stacking factor is assumed to be 0.96. The next step is to find pole arc-to-pole pitch ratio (ψ) per unit field. The range should be in range of 0.65 to 0.70.

$$\psi = \frac{\tau_p p}{\pi d} \dotfill (4.23)$$

This ratio is stated as approximation to the number of armature slots spanned by the pole arc, τ_p. The common design practice is to select a pole arc, τ_p such that:

$$\frac{\tau_p}{\lambda} = m + \frac{1}{2} \dotfill (4.24)$$

Where:

m	An integer (1,2,3,.....).
λ	Armature slot pitch (unit in inch).
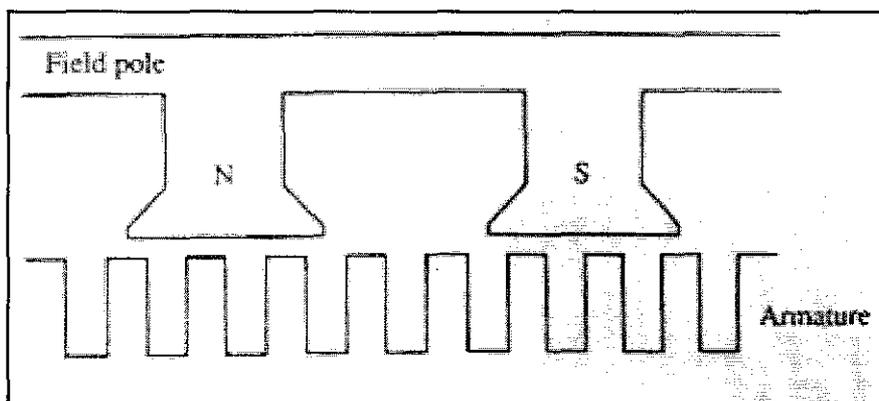
Figure 4.3: Field pole span of teeth

When equation (4.24) is satisfied, the situation per pair of poles of the dc motor is illustrated in Figure 4.3. The reluctance of magnetic circuit around a complete flux path remains nearly constant regardless of armature position. However, there can be some reluctance variation as the leading edge of a pole tip approaches a tooth while the trailing pole tip exits a tooth. This is due to different dimension of slot width and tooth width.

To ensure pole arc-to-pole pitch ratio (ψ) in the acceptable range, the value of m is selected is 9. Thus, by substituting the values, equation (4.24) becomes:

$$\frac{\tau_p}{\lambda} = 9 + \frac{1}{2}$$

$$\tau_p = 9.5 \times \lambda$$

$$= 9.5 \times 1.012 = 9.614 \, inch$$

The value of τ_p is then substitute into equation (4.23) to find pole arc-to-pole pitch ratio, ψ is shown as below:

$$\psi = \frac{9.614 \times 4}{\pi \times 17.4} = 0.703$$

These parameters finally complete the equation of apparent flux density at the tooth root, B_{tra}:

$$B_{tra} = \frac{4 \times 4.1915 \times 10^6}{0.703 \times 54 \times 0.4285 \times 7.747 \times 0.96}$$

$$= 138.588 \, kilolines \, / \, in^2$$

$$= 2.15 \, T$$

For a good design, the value of B_{tra} must be < 170 kilolines/in^2 which is equal to 2.6T (measure in Tesla). If B_{tra} is unacceptably large, action should be taken to decrease the slot width or change the number of armature slots. If an acceptable B_{tra} cannot suit the requirement, then ℓ_a must be increased. Since B_{tra} is within acceptable limits, no refinement of dimension is required.

4.3.7 Commutator design
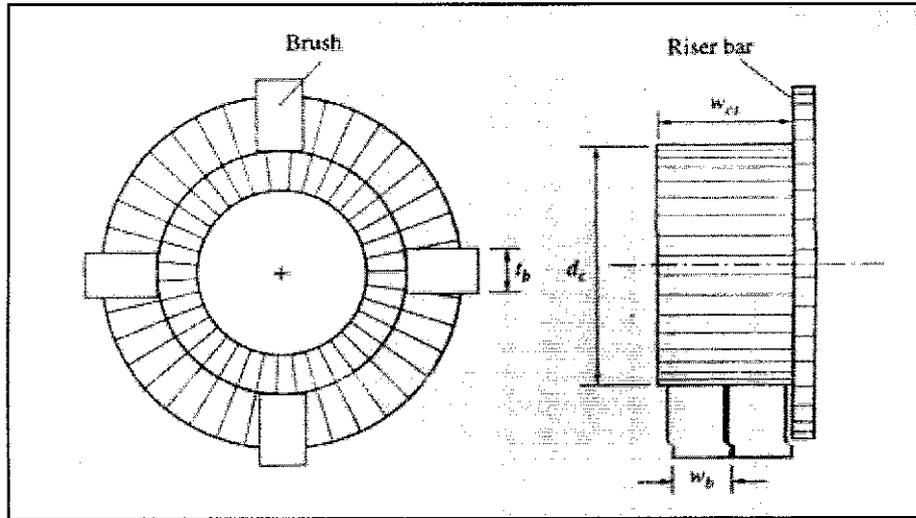
Figure 4.4: Commutator design from end view and side view

The commutator side and end view is shown in Figure 4.4. The number of commutator bars (K_c) for a two-layer winding is equal to the number of armature coils. Thus, for number of commutator bars, K_c is:

$$K_c = n_c \times N \quad\dots\dots\dots\dots\dots\dots\dots\dots\dots\dots\dots\dots \text{(4.25)}$$

Where:

n_c Number of multiple coils per slot.

N Number of armature slots.

$$K_c = 3 \times 54 = 162 \text{ bars}$$

The carbon brushes typically offer acceptable service life if the commutator surface speed does not exceed 9000 ft/min. The use of copper brushes is made for large current at low voltage machine.

Thus, the commutator brush surface diameter, d_c, should satisfy equation (4.26):

$$d_c \leq \frac{9000(12)}{\pi\, n_m} \cong \frac{34000}{n_m} \quad\dots\dots\dots\dots\dots\dots\dots\dots\dots \text{(4.26)}$$

Where:

n_m Maximum rated speed (unit in rpm).

$$d_c = \frac{34\ 000}{3\ 000} = 11.333 \text{ inch}$$

The carbon brushes should have a thickness chosen so that the brush spans $n_c + 0.5$ commutator bars insofar as standard 0.125-in increments in brush dimension allow. Thus, brush dimension, t_b is calculated using equation (4.27):

$$t_b \cong \frac{\pi\, d_c}{K_c}\left(n_c + 0.5\right) \dots\dots\dots\dots\dots\dots\dots\dots\dots\dots (4.27)$$

$$t_b \cong \frac{\pi \times 11.333}{162}\left(3 + 0.5\right) \cong 0.7692 \text{ inch}$$

As the commutator reaches the wear limit, the brush span of bars increased, thus 0.125-in increment below 0.7692 in should be selected, or use t_b =0.673 in.

Modern electro-graphite brushes exhibit life expectancy with a current density of Δ_b = 80A/in^2. The total width of n_b brushed per set is found as:

$$n_b w_b = \frac{2 I_{aR}}{p \Delta_b t_b} \dots\dots\dots\dots\dots\dots\dots\dots\dots\dots (4.28)$$

$$n_b w_b = \frac{2 \times 756.88}{4 \times 80 \times 0.673} = 7.03 \text{ inch}$$

Where:

w_b Width of a single brush. It should lies in the range 1 inch $\le w_b \le 2$ inch. For this design, w_b is assumed to be 1.5 inch.

Δ_b Brush current density for rated load (unit in A/in^2).

Once equation (4.28) being evaluated, then the number of brushes per set, n_b can be readily determined.

$$n_b = \frac{7.03}{1.50} = 4.6867 \text{ inch}$$

Therefore, the number of brushes per set, n_b is 4.6867 inch.

4.4   Field Pole Design
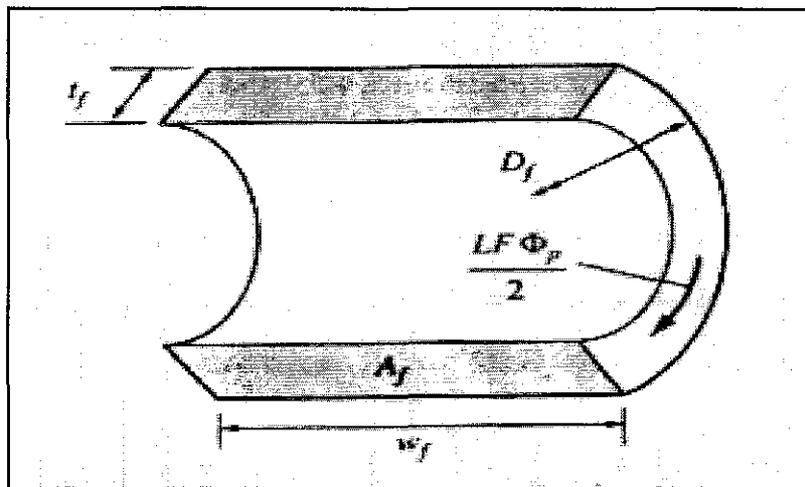
Figure 4.5: Frame section

Figure 4.5 illustrates the frame section of dc motor that associated in field pole design. Field pole design is the 3rd stage that needs to be accomplished in dc motor design. Prior to design of actual field pole, two items must be addressed which are air gap length and frame thickness. The air gap length (δ) increases with armature diameter and can be decided by:

$$\delta = 0.0335\sqrt{d} \quad\dotfill (4.29)$$

$$\delta = 0.0335 \sqrt{17.4} = 0.14 \text{ inch.}$$

Due to reluctance variation of armature teeth, the effective length (δ_e) of the air gap used in magnetic circuit calculations is greater than the tooth-to-pole face diameter determined by equation (4.30).

$$\delta_e = \frac{\lambda\,(5\delta + b_s)}{\lambda\,(5\delta + b_s) - b_s^2}\,\delta \quad\dotfill (4.30)$$

Where:

b_s Armature slot width (unit in inch).

λ Armature slot pitch (unit in inch).

δ Air gap length (unit in inch).

37

$$\delta_e = \frac{1.012\,(5 \times 0.14 + 0.45)}{\lambda\,(5 \times 0.14 + 0.45) - 0.45^2}\,0.14$$

$$= 0.17 \text{ inch}$$

The frame of a dc motor must carry 0.5 Φ_p plus any leakage flux that passes between adjacent field pole structures. The typical value for field pole leakage flux are in range of 10-20 percent of flux per pole and can be adequately accounted for with the use of leakage factor (LF) that in range of $1.1 \le LF \le 1.2$. In order to avoid an excessive mmf requirement for frame flux path, the frame flux density (B_f) should not exceed 100 kilolines/in^2. Consequently, the cross-sectional area of frame perpendicular to flux flow, A_f as illustrated by Figure 4.5 and determined using equation (4.31):

$$A_f = \frac{\frac{1}{2}LF\Phi_p}{B_f} = \frac{LF\Phi_{pR}}{200\,000} \quad\text{.........................} (4.31)$$

Where:

LF Leakage factor.

B_f Field flux density (unit in kilolines/in^2).

Since the value of Ψ is equal to 0.703 which had been determined in subsection 4.3.6-Flux density check, the field pole tips are reasonably close so that field pole leakage flux will be on the upper end of typical condition. Thus, leakage factor is chosen as LF=1.2. Thus, cross-sectional area of frame perpendicular to flux flow, A_f is as follows:

$$A_f = \frac{1.2 \times 4.27 \times 10^6}{200\,000}$$

$$= 25.62 \text{ in}^2$$

The frame can maintain a uniform thickness that extends to half of the armature coil overhang, w_f. Thus,

$$w_f = l_a + OH \quad\text{..............................} (4.32)$$

$$w_f = 7.747 + 6.5396 = 14.2866 \text{ in}$$

The necessary frame thickness, t_f is determined as:

$$t_f = \frac{A_f}{w_f} \quad \text{..} \quad (4.33)$$

$$t_f = \frac{25.62}{14.286} = 1.7933 \text{ inch}$$

With δ and t_f are determined, the height of field pole, h_p shown in Figure 4.6 can be calculated in the equation (4.34).

$$h_p = \frac{1}{2}(D_f - 2\delta - 2t_f - d) \quad \text{...........................} \quad (4.34)$$

$$h_p = \frac{1}{2}(29 - 2(0.14) - 2(1.7933) - 17.4)$$
$$= 3.8667 \text{ inch}$$

The pole shank (ℓ_{sk}) and pole shoe length (ℓ_{sh}) of field pole shape of Figure 4.6 have the reasonable values of:

$$\ell_{sk} \approx 0.9 h_p \qquad \ell_{sh} \approx 0.1\, h_p \quad \text{....................} \quad (4.35)$$

$$\ell_{sk} \approx 0.9(3.8667) \qquad \ell_{sh} \approx 0.1(3.8667)$$
$$\approx 3.48 \text{ in.} \qquad\qquad \approx 0.38667 \text{ in.}$$
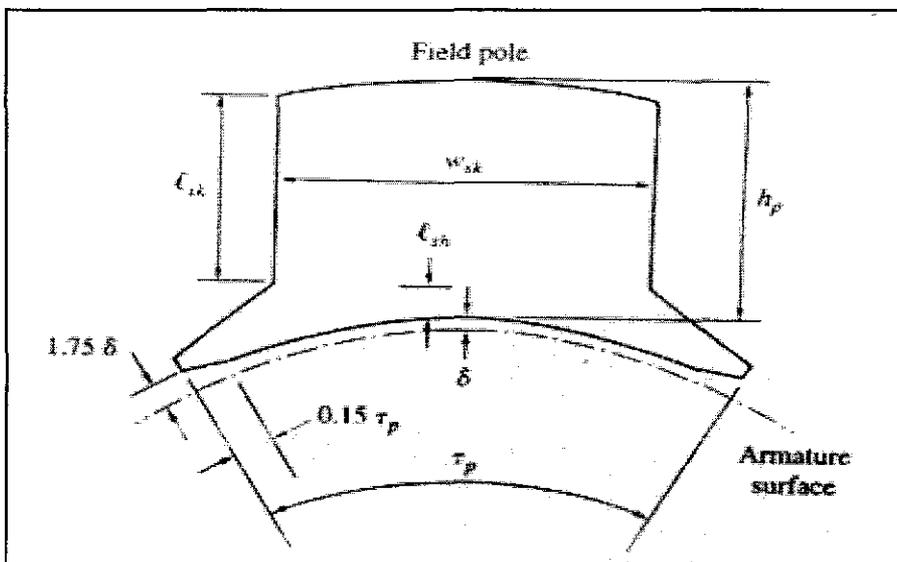
Figure 4.6: Field pole shape

Acceptable magnetic circuit performance and adequate space for the field winding usually results if the pole shank width is sized so that the flux density is 110 kilolines/in².

Hence, width of pole shank, w_{sk} is stated as below:

$$w_{sk} = \frac{LF\Phi_{pR}}{110\ 000\ l_a SF} \quad\dots\dots\dots\dots\dots\dots\dots\dots\dots\dots\ (4.36)$$

$$w_{sk} = \frac{1.2 \times 4.27 \times 10^6}{110\ 000 \times 7.747 \times 0.96}$$
$$= 6.2634\ \text{inch}$$

4.5 Magnetic Circuit Analysis

Magnetic circuit analysis is the 4th stage of dc motor design. Since the value of flux per pole, Φ_p may well be adjusted in change of operating points for a dc machine, the open-circuit saturation curve (Φ_p vs mmf_p) must be determined prior to analysis at other than the rated point. Moreover, the field winding cannot be designed for the rated point of operation until the *mmf* requirement for that point is known.

The armature teeth are tapered by nature so that the flux density at the tooth root (width w_{tr}) may experience significant saturation. When the tooth root area reaches saturation, flux tends to travel along a path radially outward and parallel to the tooth sides. A computer interface method which is MATLAB software used to computationally handle the analysis when tooth root saturation occurs. A $B_a - H$ curve for use in the tooth area analysis is constructed that accounts for parallel permeance path through slot area. It is where apparent tooth flux density (B_a) at each point is calculated as though the flux were confined only to the tooth ferromagnetic material by:

$$B_a = B + k_t H \quad\dots\dots\dots\dots\dots\dots\dots\dots\dots\dots\ (4.37)$$

The constant k_t is the permeability of the parallel air path given by:

$$k_t = 3.2\ (SF \times \lambda_3 / w_{t3} - 1)\dots\dots\dots\dots\dots\dots\dots\ (4.38)$$

Where:

λ_3 Slot pitch (unit in inch).

w_{t3} Tooth width (unit in inch).

Both parameters are calculated at one-third the tooth depth from the bottom. The MATLAB program has been formulated to calculate the necessary values and plot the magnetization curve (Φ_p vs mmf_p) for a dc machine with winding and dimensional data inserted in the program. The program assumes that the field pole and armature ferromagnetic material is M-22, 26-gage ESS and the frame is AISI 1010 steel. If the resulting magnetization curve displays saturation problem, then the offending portion of magnetic structure must be identified and corrective action taken as indicated in the Methodology section where illustrated logic flow diagram of dc motor design.

The comparing results between calculated and using MATLAB tool (<Info.m>) also included in Appendix D. Based on the result, the outcome through MATLAB provides more efficiency in term on number of decimal places compared to the calculated outcome. Although that, the differences between the results are slightly small and can be ignored.

4.5.1   B-H Curves

The <Hm22.m> and <Hx.m> programs were developed in order to perform *B-H* curves for field pole and armature ferromagnetic material is M-22, 26-gage ESS and AISI 1010 steel armature frame. With regard to the reference curves as illustrated in Figure 2.7b, some modifications were made and finally the programs were successfully run and produce the saturation curves as illustrated in Figure 4.7 and 4.8. The expected result from both programs are directly proportional curve which become constant when reach the operating point. The linear part of the curve represent the unsaturated section where else the constant part is the saturated region.

The MATLAB programs are attached in Appendix E & F and plot results are as follows.
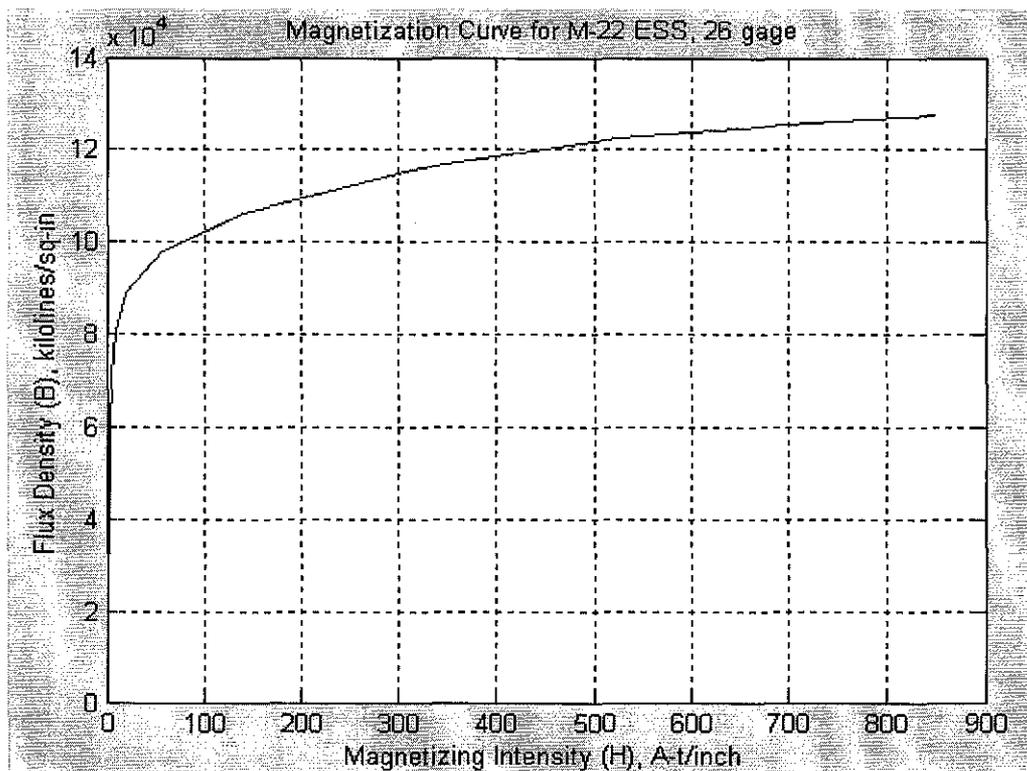
Figure 4.7: Magnetization Curve for M-22 ESS, 26 gage
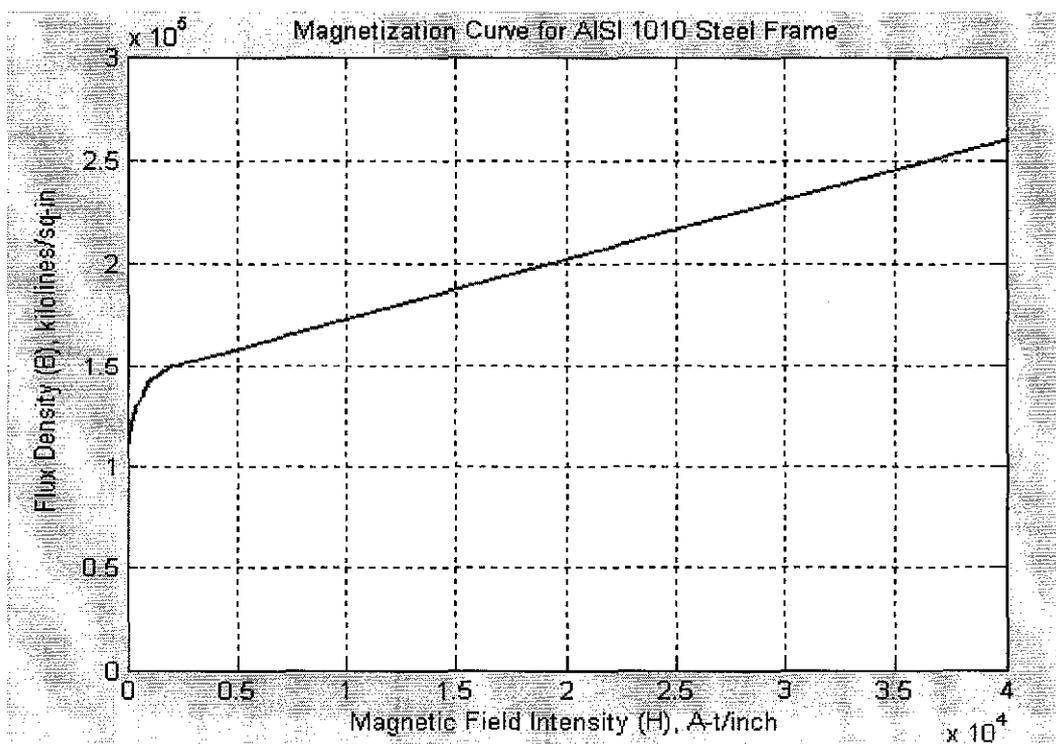
Figure 4.8: Magnetization Curve for AISI 1010 Steel Frame

4.5.2 Magnetization Curve of DC Motor

The MATLAB program <Magnetcurve.m> has been formulated to calculate the necessary values and plot magnetization curve (Φ_p vs mmf_p) for a dc machine with winding and dimensional data read from <Info.m>. Besides, the program also called the previous two programs, which are <Hm22.m> and <Hx.m> that contain the B-H curves of these two materials as illustrated in Figure 4.8 & 4.9. The MATLAB source codes are attached in Appendix G.

If the resulting magnetization curve displays saturation problem, then the offending portion of magnetic structure must be identified and corrective action should be taken as indicated by Figure 3.7: Logic flowchart of dc motor design in Methodology section. The final action taken by <Magnetcurve.m> is to form the open-circuit characteristic (OCC) curve for the dc machine and save the file for later use. OCC is a plot of no-load terminal voltage, V_t versus field current, I_f where all data is recorded for a constant value of speed. OCC indicates phenomenon known as armature reaction which means that flux per pole, Φ_p is reduced in value with regard of armature mmf F_a effect. Consideration of armature reaction is an analytical challenge owing to the nonlinearities involved. Without knowledge of armature winding data, experimental work can be conducted to determine the effects of armature reaction on the *cemf E* at several load current conditions. An experimental setup for armature reaction evaluation is illustrated in Figure 4.9. A small value of V_t may be recorded for I_f =0 owing to a slight residual magnetism present in the ferromagnetic structure. In the design, the number of field turns per pole (N_f) is not known, therefore the horizontal axis is simply plotted as field current (I_f) knowing that the result is only a scaling factor different from mmf source, F_p ($F_p=N_f I_f$). Since speed is held to a constant value for all data points, the vertical axis is only a scaling factor ($K\omega$ $=K\omega_m$) different from Φ_p. The actual value of E with armature reaction is determined by:

$$E = V_t + I_a R_a \dots\dots\dots\dots\dots\dots\dots\dots\dots\dots\dots\dots (4.39)$$

However, the setup is not being done by the student since the main concern is to develop the MATLAB program to generate such output illustrated in Figure 4.10. Figure 4.10 displays a typical plot of E vs. I_f with I_a as a parameter.

43
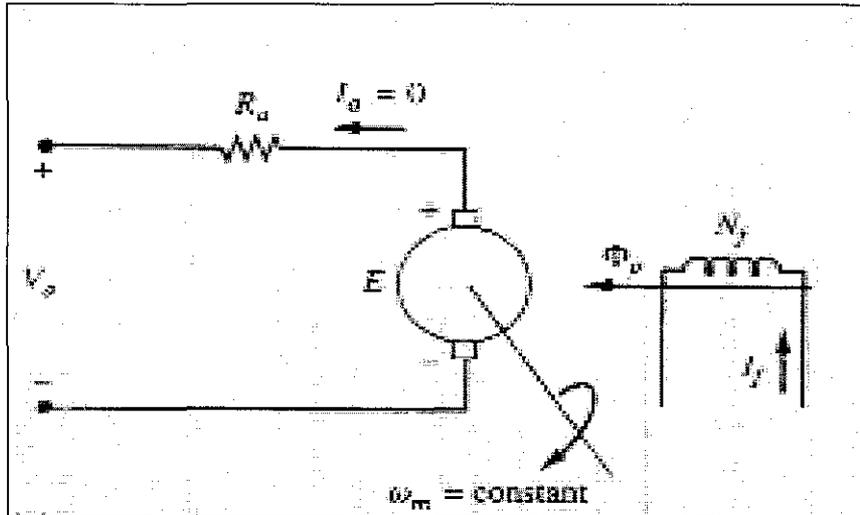
Figure 4.9: Experimental Setup for Armature Reaction Determination
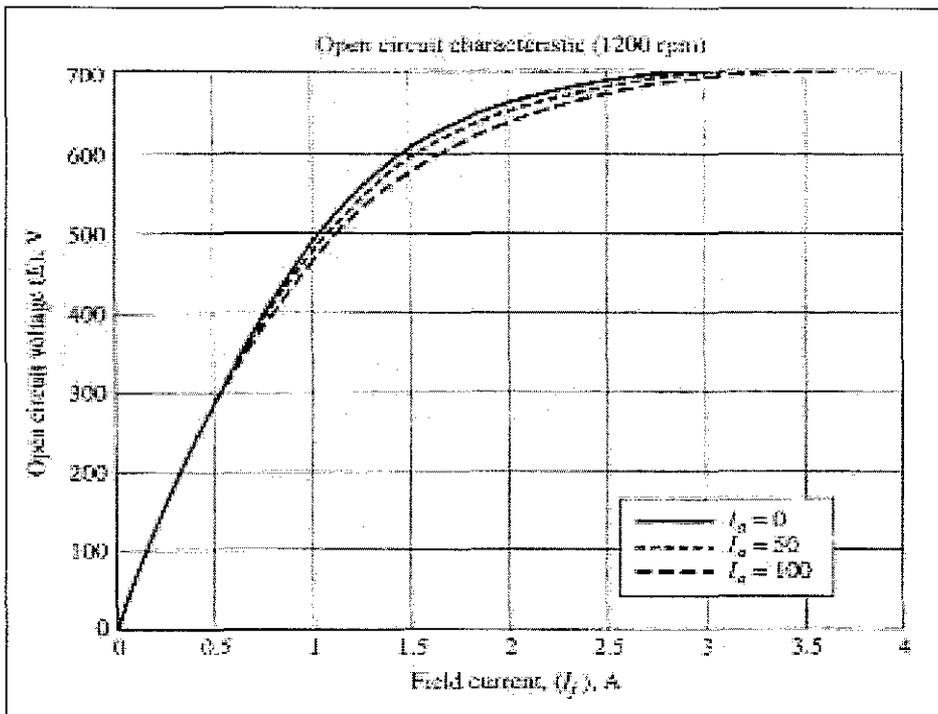
Figure 4.10: OCC Showing Armature Reaction for 1200 rpm Speed

44

Figure 4.11 illustrates magnetization curve for dc motor by including B-H curves of these two materials as illustrate in Figure 4.7 & 4.8 added with winding and dimensional data from each design stages. Figure 4.11 is used to determine the magnetomotive force (mmf_p) requirement for the rated flux per pole (Φ_p).
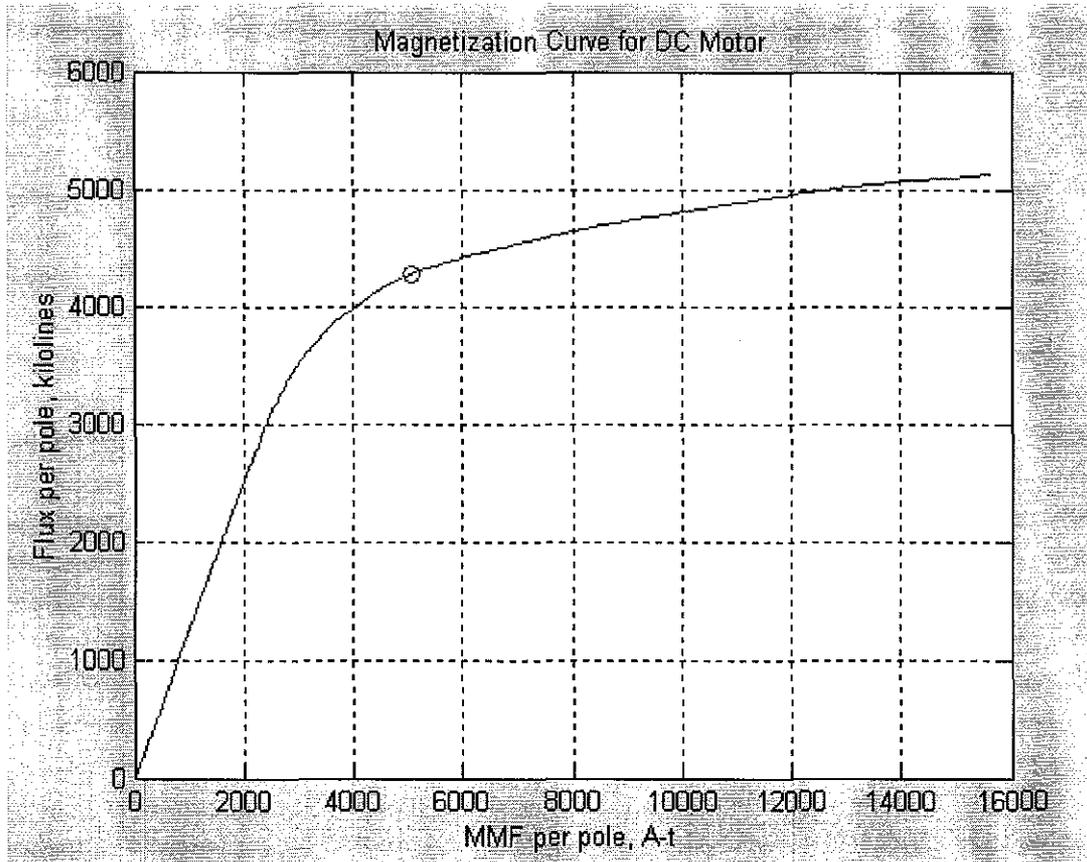
Figure 4.11: Magnetization Curve of DC Motor

4.6 Field Winding Design

Once the magnetization curve has been calculated, the value of mmf_p to produce Φ_{pR} can be determined. At least 1.05 mmf_p should be used as mmf_{pR} in field winding design to allow for armature reaction. Any field winding arrangement can be designed to produce mmf_{pR} as long as the winding physically fit into the available space surrounding the field pole. A layout drawing of field pole and frame is usually necessary to determine space availability. The space available is further diminished with the addition of the interpoles and their associated windings.

45

After execution of <Magnetcurve.m> with the values for the design entered in <Input.m>, Figure 4.11 results. Figure 4.11 illustrates magnetomotive per pole *mmf* of the dc motor design with reference of calculated flux per pole Φ_{pR} is equivalent to 4.1915 kilolines. It is found that mmf_p = 5060 A-t to produce rated flux per pole. Assuming the armature reaction increases the field *mmf* requirement by 10 percent, the shunt field should be designed to produce mmf_{pR} = (1.10)5060 = 5566 A-t. Without the benefit of a layout, it is assumed that a field winding of average width of 2.50 inch and a height of $0.85\ell_{sk} \cong 0.85(3.48) \cong 2.96$ inch can be fitted into the interpolar space. The area of the field winding cross section is (2.50)(2.96) = 7.40 in^2. If No. 14 square wire insulated with heavy film over double glass is selected for the field conductor, 1100 turns (N_f) can be fitted into the available area.

The mean length turn of the field winding, MLT_f is:

$$MLT_f = 2\left[l_a + w_{sk} + 2(2.5)\right] \dots\dots\dots\dots\dots\dots (4.40)$$

$$MLT_f = 2\left[7.747 + 6.2634 + 2(2.5)\right]$$

$$= 38.02 \ inch$$

Where:

ℓ_a Armature stack length

w_{sk} Width of pole shank

No. 14 square magnet wire has a resistance of 5.25 Ω per 1000 ft for a temperature of 160°C. Thus, the resistance per pole, R_{fp} is:

$$R_{fp} = \frac{N_f MLT_f}{1000(12)}(5.25) = \frac{1100(38.02)}{1000(12)}(5.25) = 18.2971 \ \Omega$$

Where:

N_f Number of field turns

MLT_f Mean length turn of the field winding

For a series connection of all field poles, R_f:

$$R_f = pR_{fp} = 4(18.2971) = 73.1885 \ \Omega$$

Where:

R_{fp} Field resistance per pole

p Number of poles

Full voltage across the field winding yields field current, I_f of:

$$I_f = \frac{V_t}{R_f} = \frac{415}{73.1885} = 5.6703 \ A$$

$$mmf_p = N_f I_f = 1100(5.6703) = 6237.3187 \ A-t$$

Where:

V_t Rated Terminal Voltage

R_f Field resistance of a series connection

mmf_p Magnetomotive per pole

It is concluded that this field winding can adequately excite the motor for the rated point of operation.

4.7 Performance Analysis

The design stages continued by performing MATLAB program to analyze the performance of this motor design. The program clearly indicate how the performance of design towards the specification given by the customer.

The program <Shunt.m> is formulated with use of OCC that has been saved by <Magnetcurve.m> to plots the speed-torque, speed-armature current, speed-output power and speed-efficiency curves for the motor design to allow assessment with regard to performance specifications. If the motor does not meet the desired performance, thus the design must be iterated as indicated in Figure 3.1. <Shunt.m> is the final program in this design project. This program is collaboration with the previous source codes and merely depends on each successful execution of all above programs. The program is attached in Appendix H.

47

4.7.1 MATLAB Outcomes for Performance Analysis

<Shunt.m> develop torque-speed, speed-line current, speed-output power and speed-efficiency analysis curves for shunt excited dc motor with rated voltage applied. Armature reaction is neglected in this program. The complete MATLAB program for the analysis is attached in Appendix H. Figure 4.14, Figure 4.15, Figure 4.16 and Figure 4.17 illustrate the analysis of dc motor based upon the performance specification.
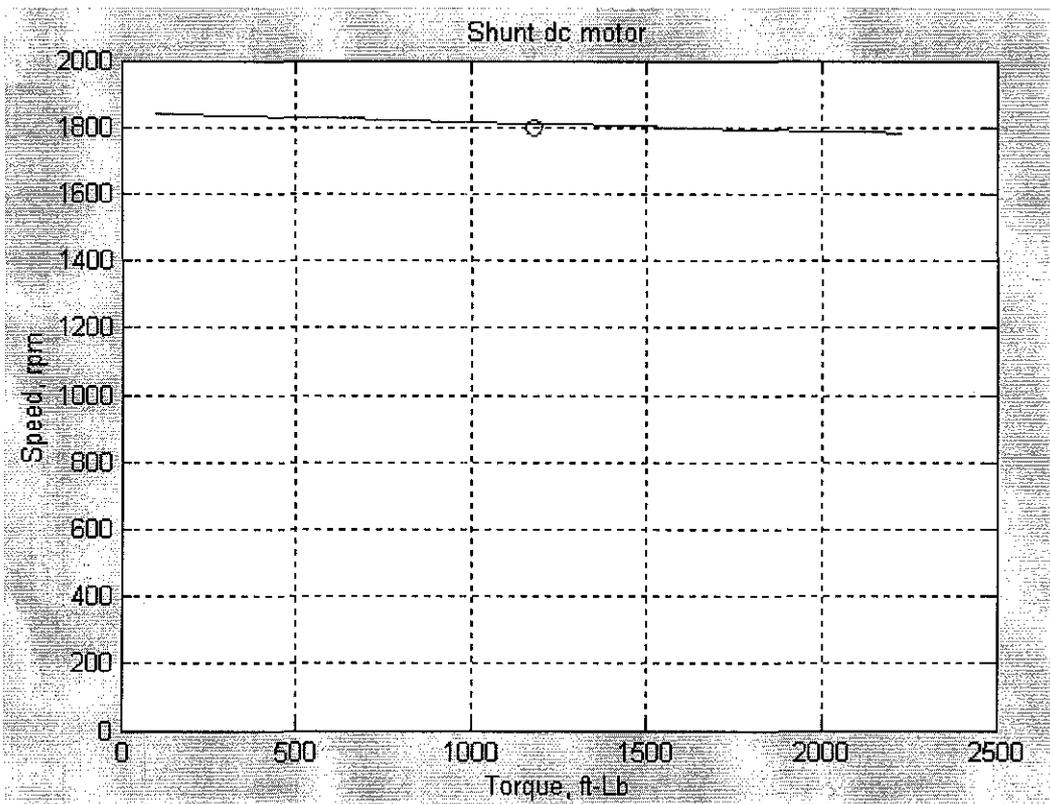
Figure 4.12: MATLAB Speed versus Torque Curve
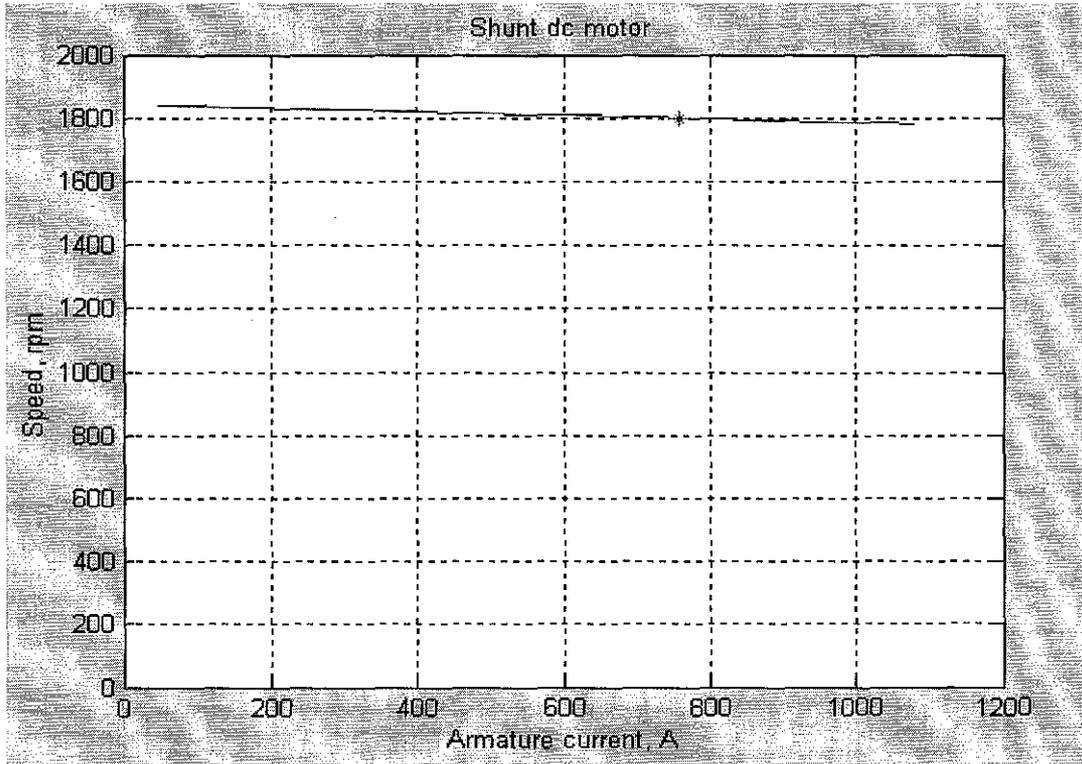
Figure 4.13: MATLAB Speed versus Armature Current Curve
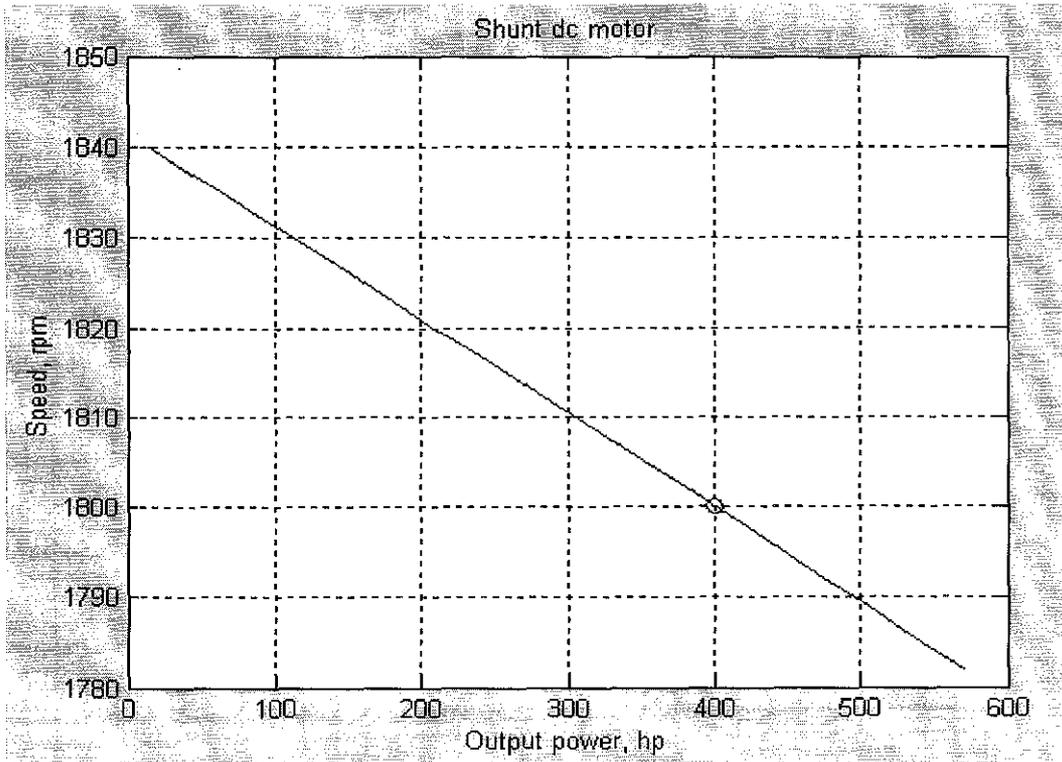
Figure 4.14: MATLAB Speed versus Output Power Curve

49
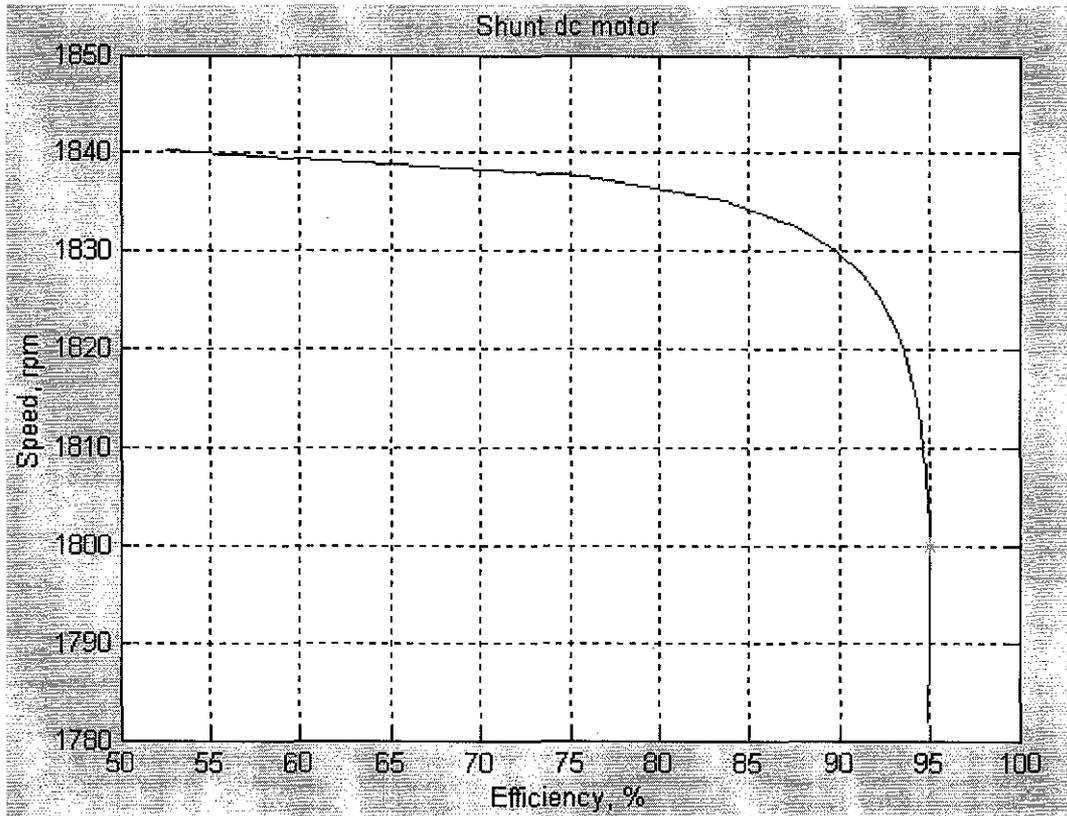
Figure 4.15: MATLAB Speed versus Efficiency Curve

4.8   Discussion

The main purpose of designing dc motor studies is to provide an accurate shunt excited dc motor design with regard to performance specification given by the user. In this project, the designing stages started with volume and bore sizing and ended with design refinement or performance analysis. All the required parameters in every design stages are calculated and the values are being used in MATLAB as data input of the programming. The analysis part where the plot-curves become the main element is accomplished using an interactive computer software, MATLAB programming. The MATLAB programs are mainly comprise of specifications given by the customer, set of commands and relevant functions, the equations for performing data input and also added in small portion of C++ coding.

All dc motors must receive their excitation from an outside source or independent source; therefore, they are separately excited. Their field and armature windings are connected, however, in one of three different ways employed for self excited dc generators. Thus, according to the field arrangement, there are three types of dc motors namely:

1. Series Wound.
2. Shunt Wound.
3. Compound Wound.

For this design, the field arrangement selected is shunt excited dc motor. The shunt dc motor arrangement is illustrated in Figure 4.16. A shunt wound motor is one in which field winding consisting large number of turns of comparatively fine wire connected in parallel with armature circuit. The field current of the motor gets its power directly across the armature terminals of the motor.
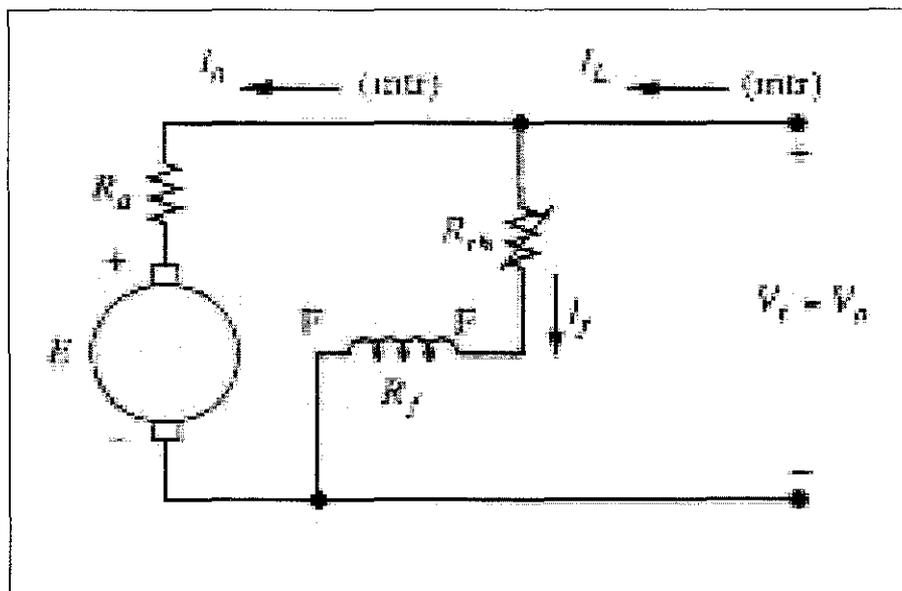
Figure 4.16: Shunt DC Motor Equivalent Circuit

4.8.1 Motor Characteristic

The important characteristic curves of dc motor are:

1. Speed-Torque Characteristic: This curve gives relationship between speed at rated load n_{mR} and developed rated torque τ_{dR}.

2. Speed-Armature Current Characteristic: The characteristic curve gives relationship between speed at rated load n_{mR} and armature current I_a.

3. Speed-Output Power Characteristic: This curve gives relationship between speed at rated load n_{mR} and output power P_{out}.

4. Speed-Efficiency Characteristic: The curve gives relationship the efficiency η_R of the design with respect to the speed n_{mR}.

4.8.2 DC Shunt Motor Performance

For this study, the motor performance is based on a constant value of impressed terminal voltage. In such a case, the field voltage remains constant for the shunt dc motor so that its field current remains constant, rendering its performance nature identical to the separately excited dc motor.

Applying Kirchoff's Voltage Law (KVL) to the equivalent circuit of Figure 4.13 and solving for speed ω_m gives:

$$\omega_m = \frac{V_a - I_a R_a}{K\Phi_p} \quad \text{.. (4.41)}$$

The expression of (4.41) yields the motor shaft speed regardless of the field connection. For the case of a shunt motor, $V_a = V_t$. The motor shaft torque τ_s is given by:

$$\tau_s = \tau_{dR} - \tau_{FW} = K\Phi_p I_a - \frac{P_{FW}}{\omega_m} \quad \text{.......................... (4.42)}$$

Where:

τ_{FW} Friction and windage torque

τ_{dR} Developed rated torque

K Constant depend on the construction of a particular DC machine

I_a Armature Current

Φ_p Flux per pole

ω_m Motor Speed

P_{FW} Mechanical rotational losses

In many power conditioned drives, the field winding may be excited from an independent source as mentioned earlier. This is where the field current is controlled to allow versatility in performance such as shaping torque or power profiles as functions of motor speed. Figure 4.14 presents the general power flow diagram for a dc motor. For the case of shunt motor, $P_{in} = V_t I_a + V_f I_f$. Any core losses are lumped with the mechanical rotational losses, P_{FW}.

4.8.3   Speed-Torque Characteristic Curve

Figure 4.14 results a straight line with negative slope for this analysis. When the rated speed n_{mR} is 1800 rpm, the developed torque τ_{dR} is 1228.07 ft-lb. This result meets the design specification due to the fact that the indicated value is the same compared to the calculated using equation (4.1). For a shunt dc motor to respond with the load, the load on the shaft of a motor is supposedly increased. Then the rated developed torque, τ_{dR} will exceed the induced torque τ_{ind} in the machine, and the motor will start to slow down. When the motor slows down, its internal generated voltage drops ($E_a = K\Phi_p\omega_m$) decreases, thus the armature current in the motor I_a increases. As the armature current rises, the induced torque in the motor increases ($\tau_{ind} = K\Phi_p I_a$), and finally the induced torque will equal to the rated developed torque at a mechanical speed of rotation ω_m.

The output characteristic of a shunt dc motor can be derived from the induced voltage and torque equations of the motor plus Kirchhoff's voltage law. The KVL equation for a shunt motor is indicated in (4.43):

$$V_t = E_a + I_a R_a \dots\dots\dots\dots\dots\dots\dots\dots\dots (4.43)$$

The induced voltage $E_a = K\Phi_p\omega_m$, so (4.43) is expressed as:

53

$$V_t = K\Phi_p \omega_m + I_a R_a \dots\dots\dots\dots\dots\dots\dots\dots\dots\dots\dots (4.44)$$

Since $\tau_{ind} = K\Phi_p I_a$, armature current I_a can be expressed as:

$$I_a = \frac{\tau_{ind}}{K\Phi_p} \dots\dots\dots\dots\dots\dots\dots\dots\dots\dots\dots\dots\dots (4.45)$$

Combining equation (4.44) and (4.45) produces:

$$V_t = K\Phi_p \omega_m + \frac{\tau_{ind}}{K\Phi_p} R_a \dots\dots\dots\dots\dots\dots\dots\dots\dots\dots (4.46)$$

Finally, solving for the motor's speed yields:

$$\omega_m = \frac{V_t}{K\Phi_p} - \frac{R_a}{(K\Phi_p)^2} \tau_{ind} \dots\dots\dots\dots\dots\dots\dots\dots\dots (4.47)$$

Where:

V_t Terminal Voltage

E_a Internal generated voltage

R_a Armature Resistance

τ_{ind} Induced Torque

τ_{dR} Developed Rated Torque

This equation indicates that the result is a straight line with a negative slope. In order to the speed of the motor to vary linearly with torque, the other terms in this expression must be constant as the load changes. The terminal voltage supplied by the dc power source is assumed to be constant. If it is not constant, then the voltage variations will affect the shape of the torque-speed curve. Consequently, in shunt dc motor case the flux is considered to be constant and thus will increase torque as the load current keep increasing which leads to reduction in Φ_p. Owing to the relative sizes of the two terms of (4.43), their difference will increase in value, or the motor speed increases for a particular value of τ_{dR}.

Accordingly, the torque-speed curve of Figure 4.14 would display less speed droop if armature reaction were considered. Stated in term of speed regulation, armature reaction

can reduce the speed regulation of a dc shunt motor. If a shunt motor is operating with a weak shunt field, armature reaction can reduce Φ_p sufficiently so that the loaded exceeds the unloaded speed, giving a negative value of speed regulation. On the other hand, the current is remains constant as well as speed of the motor.

4.8.4   Speed-Current Characteristic Curve

The shunt dc motor speed-current curve which is illustrated Figure 4.15 exhibits the nearest value to a constant speed characteristic of all dc motor configurations when no control of field current is exercised. When the speed is at 1800 rpm, the armature current is 756.88 A. By rearrange the equation (4.43), the armature current I_a become independent variable as indicate below:

$$I_a = \frac{V_t - E_a}{R_a} \dots\dots\dots\dots\dots\dots\dots\dots\dots\dots\dots\dots\dots\dots\dots (4.48)$$

Armature resistance R_a and terminal voltage V_t are considered constant in this analysis, thus the curves only affected with the changes of internal generated voltage E_a with the respect to armature current I_a. When the motor slows down, its internal generated voltage drops $(E_a = K\Phi_p\omega_m)$ decreases, therefore the armature current in the motor I_a increases drastically in wide range as illustrate in Figure 4.15.

The applied voltage V_t is kept constant, so that the field current is remain constant. Hence, flux per pole Φ_p will have maximum value on no load and will decrease slightly due to armature reaction as the load increases. However, in this study the flux is considered to be constant and the armature reaction's effect is neglected. From the expression of speed, n_{mR} is directly proportional to back e.m.f. E_b or $(V_t - I_aR_a)$ and inversely proportional to the flux Φ_p. Since the flux is considered to be constant as mentioned above, therefore with increasing in armature current, the speed slightly falls due to increase in voltage drop in armature circuit.

In view of the fact that there is a slight variation in speed of the shunt motor from no load to full load and this slightly variation in speed can be made up by inserting resistance in the shunt field and thus reducing the flux. As a result, shunt motor can be used for loads which are totally and suddenly thrown off without ensuing in excessive speed. Shunt motor being constant speed motor is best suited for driving of line shaft, machine lathe, milling machine, conveyor, fan and for all purposes where constant speed is required. It is not suitable for use with flywheel or with fluctuating loads or for parallel operation due to its constant speed characteristic.

4.8.5   Speed-Output Power Performance Curve

From speed-rated output power curve illustrated in Figure 4.16, the design motor produces an output power of 400 hp when the rated speed of 1800 rpm. The equation (4.49) defines the relationship between speed and output power.

$$P_{out} = \tau_{dR}\omega_m \quad\dotfill (4.49)$$

For this analysis, the output power P_{out} is increased when developed rated torque τ_{dR} increases and the motor speed ω_m decreases. The analysis is true based on rearranging equation (4.49) which results:

$$\tau_{dR} = \frac{P_{out}}{\omega_m} \quad\dotfill (4.50)$$

Hence, the design meet the specification given as the motor produce the rated output power of 400 hp when the motor's speed is 1800 rpm. DC motor is used where a substantially constant speed is required as the machine shop drives.

4.8.6 Speed-Efficiency Performance Curve

MATLAB program also produced the efficiency curve of Figure 4.17 for 400-hp dc shunt motor over the load torque range from a small value to approximately 150 percent of rated torque. From Figure 4.17, it is noted that the efficiency of shunt motor at rated speed of 1800 rpm successfully meet the specified design goal of 95 percent. This relationship is best described by equation (4.51):

$$\eta_R = \frac{P_{out}}{P_{in}} \quad\text{... (4.51)}$$

Input power P_{in} is assumed to be constant, thus the efficiency of the motor is increases as the output power P_{out} also increases. As mention earlier, with increasing of P_{out} the speed will drop respectively. So, when the speed decreases in small variation, the efficiency is rapidly increases in wide range of values.

The efficiency remains above 90 percent for the developed rated torque that approximately above 50 percent of the rated value. However, it drops off characteristically for light loads as the near constant rotational and field winding become comparable to the output power in value. The armature copper loss varies as the square of the current, so this loss termed as variable loss. The efficiency of the shunt motor becomes high when variable loss is equal to the constant loss. For this shunt motor case of near-constant speed and voltage operation, any core losses of the armature have been absorbed in the P_{FW} value.

CHAPTER 5

CONCLUSION AND RECOMMENDATION

In the late 1800s, several inventors built the first working motors, which used direct current (DC) power. After the invention of the induction motor, alternating current (AC) machines largely replaced DC machines in most applications. However, DC motors still have many uses and demands from customer. Due to its outstanding capability, a good and significant design of dc motor is essential in order to meet customer's requirement. The design phases definitely require several stages from calculating the developed torque until formulating MATLAB program to produce the required analysis. The analysis from MATLAB with regard to performance specifications given by the customer will reflect the accuracy of overall design procedures.

Shunt motors use high resistance field windings connected in parallel with the armature. By varying the field resistance, it changes the motor speed. Shunt motors are prone to armature reaction, a distortion and weakening of the flux generated by the poles that result in commutation problems evidenced by sparking at the brushes. Installing additional poles, called interpoles, on the stator between the main poles wired in series with the armature reduces armature reaction. DC motors are classified or identified according to the field winding connection.

Significantly different torque-speed characteristics are exhibited by dc motors depending on the field winding connection configuration chosen. The characteristic curve displays a less speed drop when increasing the torque if armature reaction were considered. Speed-current characteristic curve exhibits the nearest value to a constant speed characteristic when no control of field current is exercised. For speed-output power, the design is accurately meet the requirement where for speed of 1800 rpm, the output power is 400 hp. The assessment of speed-efficiency curve is correct as it meet the performance requirement. As the conclusion, the objectives of this project have been successfully achieved and the use of MATLAB in magnet circuit and performance analysis was found to be very applicable, imperative and beneficial.

As a recommendation, the project on designing shunt dc motor can be improved by adding graphical user interface or GUI as the main interface to the customer to insert any specifications desired and will automatically generate the correct performance analysis for the design machine. A graphical user interface (GUI) is a user interface built with graphical objects, such as buttons, text fields, sliders, and menus. In general, these objects already have meanings to most computer users. Applications that provide GUIs are generally easier to learn and use since the person using the application does not need to know what commands are available or how they work. The action that results from a particular user action can be made clear by the design of the interface. Thus, by implementing GUI, the user can make any changes or modification to the specification which in turn will result different plot-curves analysis. This will ease the user to do comparison on dissimilar machine design and choosing the appropriate design based upon their application's requirement.

The project can be improved by implement the actual prototype of the dc motor design. This only can be done if all the necessary equipments are provided. The mechanical design of the motor can be tested whether it meet the requirement based on MATLAB analysis. By implementing both hardware and software, the accuracy of the design is increased and can fully satisfy the user's requirement.

REFERENCES

[1]   G.R. Slemon and A. Straughen, *Electric Machines,* Addison-Wesley Publishing Company, New York, 1982.

[2]   David R. Carpenter, *Electrician's Technical Reference (Motors),* Delmar Publishers, New York, 1998.

[3]   R.K. Rajput, *Direct Current Machines,* Laxmi Publications (P) Ltd, New Delhi, 1993.

[4]   Stephen J. Chapman, *Electric Machinery and Power System,* McGraw-Hill Publishing Company Limited, New York, 2002.

[5]   I J Nagrath and D P Kothari, *Electrical Machines Second Edition,* Tata McGraw-Hill Publishing Company Limited, New Delhi, 1997.

[6]   Chee-Mun Ong, *Dynamic simulation of Electric Machinery Using MATLAB/ Simulink,* Prentice Hall Ptr, New Jersey, 1998.

[7]   Kenneth R. Demarest, *Engineering Electromagnetics,* Prentice Hall Ptr, New Jersey, 1998.

[8]   Steven J. Marrano and Craig DiLouie, *Electrical System Design & Specification Handbook For Industrial Facilities,* The Fairmont Press Inc, GA,1998.

[9]   L.O. Dallin, *BTS1 Septum Magnets,* CLS Design Note-2.1.41 Rev.0, University of Saskatchewan Saskatoon, Canada, 2000.

[10]   J.B. Gupta, *Theory & Performance of Electrical Machines,* SSMB Publishing Division, India, 1997.

[11]   The MathWorks. *MATLAB Student Version Learning MATLAB 6* (Release 12), 2nd printing, New York, 2001.

[12]   http://www.electricmotorwarehouse.com/NEMA_frame_info.htm

[13]   http://www.google.com/dc_machine/design_consideration.htm

[14]   http://www.mathworks.com/access/helpdesk/help/techdoc/learn_MATLAB/ch 1intro.shtml#12671

[15]   http://www.mathworks.com/access/helpdesk/help/pdf_doc/ MATLAB/ using_ml.pdf

APPENDIX A
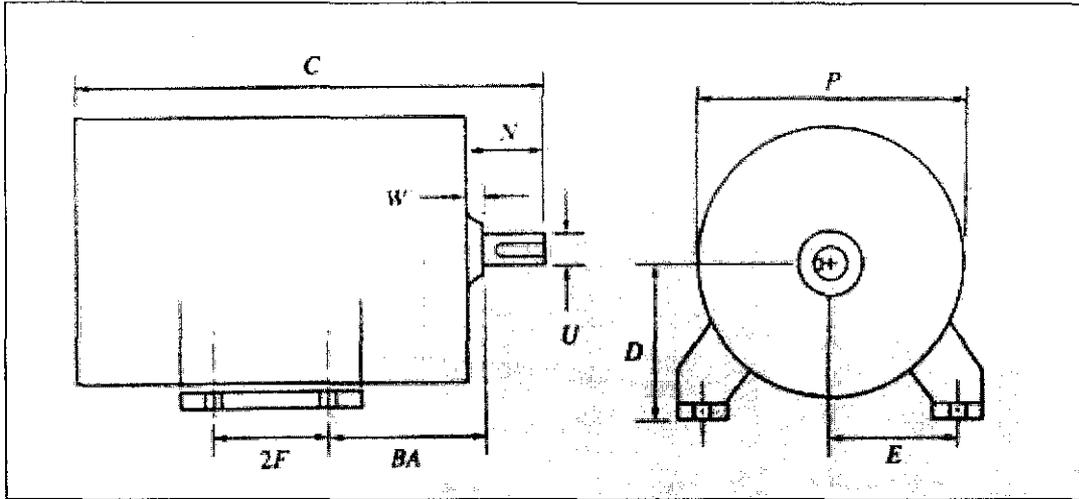
Basic NEMA Frame Dimension

Frame designation	C	N-W	U	2F	BA	P	D	E
168AT	15.88	1.75	0.875	8.00	3.25	7.88	4.00	3.25
188AT	19.25	2.25	1.125	9.00	2.75	9.50	4.50	3.75
219AT	22.75	2.75	1.375	11.00	3.50	11.00	5.25	4.25
258AT	26.62	3.25	1.625	12.50	4.25	13.00	6.25	5.00
288AT	30.75	3.75	1.875	14.00	4.75	14.00	7.00	5.50
323AT	27.62	4.25	2.125	9.00	5.25	16.00	8.00	6.25
365AT	33.12	4.75	2.375	12.25	5.88	18.00	9.00	7.00
405AT	36.00	5.25	2.625	13.75	6.62	20.00	10.00	8.00
505AT	50.12	6.50	3.250	18.00	8.50	25.00	12.50	10.00
583AT	**53.62**	**7.50**	**3.750**	**16.00**	**10.00**	**29.00**	**14.50**	**11.50**
687AT	68.38	9.50	4.500	32.00	10.00	29.50	14.50	11.50
688AT	72.88	9.50	4.500	36.00	11.50	35.00	17.00	13.50

NEMA Frame Designation (unit in inch)

APPENDIX B

DC Machine Sizing Value

DC machine sizing value

APPENDIX C

```
                    ┌──────────────────┐
                    │  Specification   │
                    └──────────────────┘
                             │
                             ▼
              ┌──────────────────────────┐        No
              │  Armature diameter and   │◄──────────────────┐
              │      length sizing       │                   │
              └──────────────────────────┘                   │
                             │                                │
                             ▼                                │
              ┌──────────────────────────┐              ╱─────────────╲
         ┌───►│ Select no. armature slots│     Yes     ╱  Select new   ╲
         │    │                          │◄───────────▕ armature slot?  ▏
         │    │  Size armature slot and  │             ╲               ╱
         │    │        conductor         │              ╲─────────────╱
         │    └──────────────────────────┘                    ▲
         │                  │                                  │
         │                  ▼                                  │
         │         ╱─────────────────╲                        │
      No │        ╱     Armature       ╲                      │
         └───────▕   current density    ▏                     │
                  ╲                     ╱                      │
                   ╲───────────────────╱                      │
                             │                                │
                             ▼  Acceptable                    │
                    ╱─────────────────╲          No           │
                   ╱   Tooth root flux  ╲──────────────────────┘
                  ▕       density        ▏
                   ╲                    ╱
                    ╲──────────────────╱
                             │
                             ▼  Acceptable
              ┌──────────────────────────┐
              │    Commutator design     │
              └──────────────────────────┘
                             │
                             ▼
              ┌──────────────────────────┐
              │    Field pole design     │
              └──────────────────────────┘
```
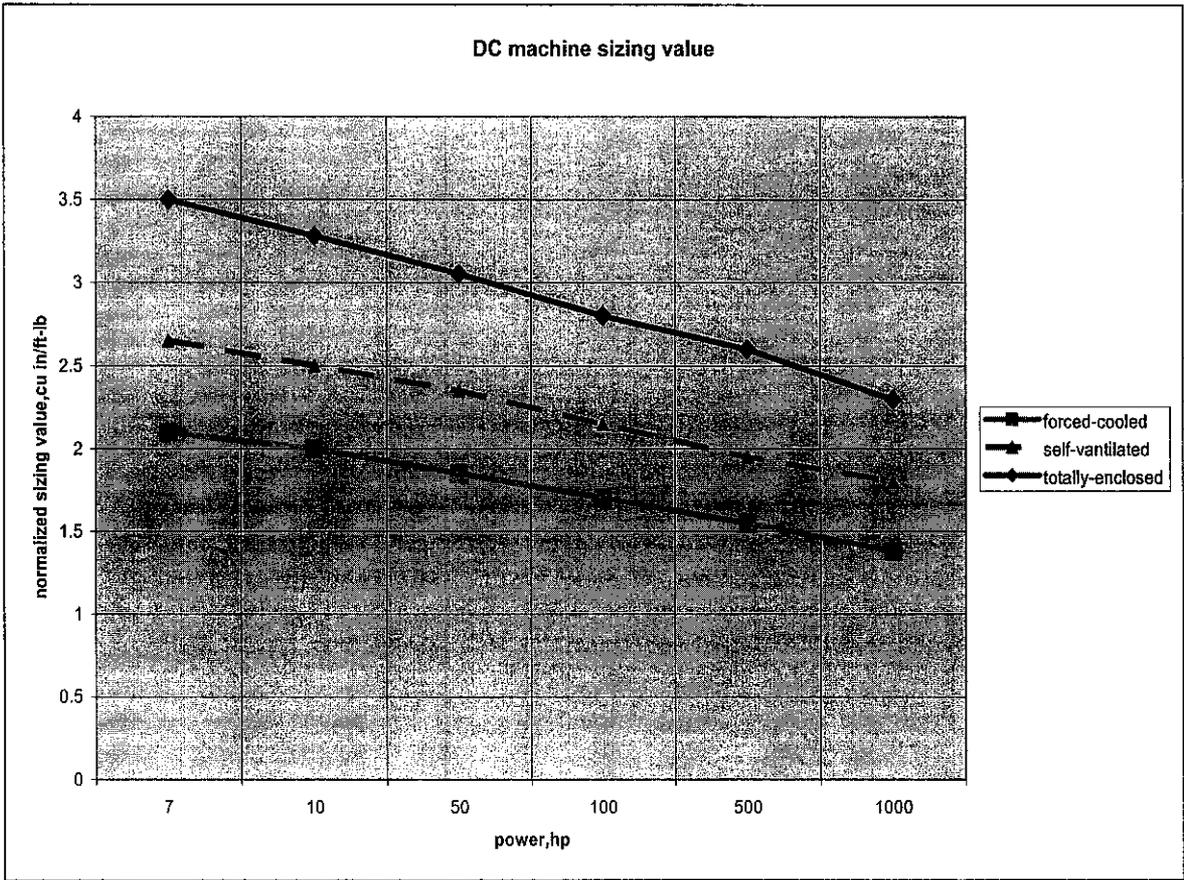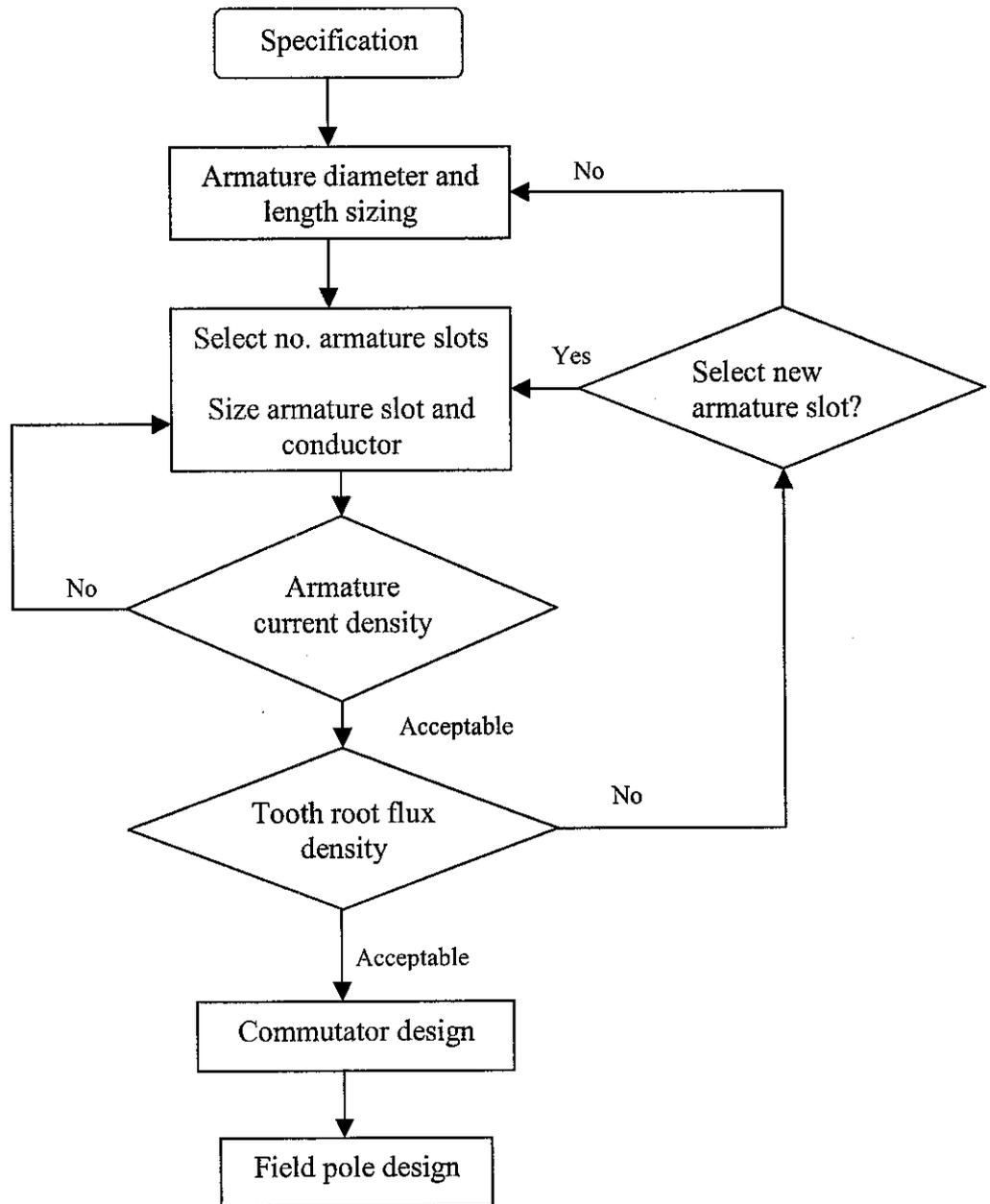
Logic flowchart for armature design

APPENDIX D

MATLAB Source Codes for Data Input of DC Motor

```
%Specification of dc motor
VtR=415;              %Rated terminal voltage(V)
PsR=400;              %Rated power(hp)
nmR=1800;             %Rated speed(rpm)
eTaR=0.95;             %Efficiency
f=50;                 %Frequency(Hz)
nmax=3000;            %Maximum speed(rpm)
p=4;                  %Number of pole


%1st stage:Volume and bore sizing
%Set armature diameter(d)
Df=29;        %Outside frame diameter. From NEMA dimension,P=Df=29 inch.
d=0.6*Df;     %d in range of 0.55Df<d<0.65Df. Choose midrange(0.6Df)
%Rated developed torque(ft.Lb). Assumption of 5% rotational losses.
TdR=5250*PsR/0.95/nmR;
%Armature stack length(la)
vT=1.91;              %Normalized sizing value;taken from dc sizing value
la=vT*TdR/d^2;        %Unit in inch


%2nd:Armature Design
%Number of armature slots(N)
lambda1=1;
N1=pi*d/lambda1;
N=54;                 %N must be an even number,thus choose N=54
lambda=pi*d/N;        %Armature slot pitch(inch)
%Voltage and torque constant(kE and kT)
nc=3;                 %Number of coils per slot
Z=2*nc*N;             %Total conductor of armature winding
a=4;                  %Number of lap winding(consider simplex,a=p)
kE=p*Z/(a*60*10^8);     %Unit in V/lines.rpm
kT=p*Z/(a*8.525*10^8);  %Unit in ft.Ib/lines.A
```

%Rated current and flux per pole(IaR & phiR)

IaR=746*PsR/eTaR/VtR   %Unit in Ampere

phiR=TdR/kT/IaR;   %Unit in Megalines

%Slot design

bs=0.45;   %Armature slot width for irregularity material

ds=1.15;   %Slot depth for irregularity material

triA=4200;   %Self-ventilated machine fall in midrange of 3200<triA,5200 A/in^2

sa=IaR/a/triA;   %Armature conductor area (in^2)

wc=0.110;   %To have bs in midrange(0.4<bs<0.5), select armature conductor with bare copper width(wc)=0.11

dc=sa/wc;   %Conductor height(inch)

%Coil characterization

%Complete end-turn overhang(OH)

se=0.125;   %Slot wedge

be=0.5;

ge=ds;

de=se+bs;

lambdaC=pi*(d-ds)/N;

alpha=asin(de/lambdaC);

tC=(N/p)*lambdaC;

fe=(tC/2)*tan(alpha);

OH=be+fe+ge;

%Mean-length turn of armature coil(MLTa)

x=tC/cos(alpha);

y=2*be;

z=2*ge;

MLTa=2*(x+y+z+la);

%Armature resistance(Ra)

T=150;   %Average conductor temperature(degC)

rho=((234.5+T)/254.5)*0.69*10e-7;

Ra=(rho*MLTa*Z/2)/a^2/sa

```
%Flux density check(Btra)
wtr=(pi*(d-2*ds)/N)-bs;
tp=9.5*lambda;
chi=p*tp/pi/d;   %Field pole arc-to-pole pitch ratio
SF=0.96;
q=chi*N*wtr*la*SF;
Btra=phiR*p/q;


%Commutator design
%Number of commutator bars(Kc)
Kc=nc*N;
%Average volts per bar(ecav)
ecav=VtR*p/Kc;
%Commutation dimension
dc=34000/nmax;
%Brush dimension(tb)
tb=(pi*dc/Kc)*(nc+0.5);
%Total width of nb brushes per set(nbwb)
triB=80;        %Electrograhitic brushes current density(A/in^2)
nbwb=(2*IaR)/p/triB/tb;


%3rd stage:Field pole design
%Air gap length
delta=0.0335*sqrt(d);
%Cross-sectional area of fame perpendicular to flux flow
LF=1.2;        %Leakage factor(1.1<LF<1.2)
Af=LF*phiR/200000;
wf=la+OH;
tf=Af/wf;         %Frame thickness
hp=0.5*(Df-2*delta-2*tf-d);    %Height of field pole
lsk=0.9*hp;    %Pole shank
lsh=hp-lsk;    %Pole shoe length
%Field pole width
wsk=(LF*phiR)/110000/la/SF;
```

```
>> info
d =
        17.4000
TdR =
        1.2281e+003
Ia =
        7.7474
N1 =
        54.6637
lambda =
        1.0123
Z =
        324
kE =
        5.4000e-008
kT =
        3.8006e-007
IaR =
        756.8802
phiR =
        4.2692e+006
sa =
         0.0451
wc =
         0.1100
dc =
        0.4096
ge =
        1.1500
de =
        0.5750
lambdaC =
        0.9454
alpha =
        0.6538
```

tC =

   12.7627

fe =

   4.8896

OH =

   6.5396

x =

   16.0786

y =

   1

z =

   2.3000

MLTa =

   54.2521

rho =

   1.0425e-006

Ra =

   0.0127

wtr =

   0.4285

tp =

   9.6168

chi =

   0.7037

q =

   121.1005

Btra =

   1.4101e+005

Kc =

   162

ecav =

   10.2469

dc =

   11.3333

tb =

   0.7692

triB =

   80

nbwb =

   6.1496

delta =

   0.1397

Af =

   25.6151

wf =

   14.2871

tf =

   1.7929

hp =

   3.8674

lsk =

   3.4806

lsh =

   0.3867

wsk =

   6.2619

APPENDIX E

MATLAB Source Codes of Magnetization Curve for M-22 ESS, 26-gage

\<Hm22.m\>   B-H interpolation routine

```
function y=Hm22(Bx)
%Hm22 is field pole and armature ferromagnetic material(M-22, 26-gage ESS)
% B-H values that follow are valid for M-22, 26 ga. ESS
B=[0 0.4 0.8 2 8 9.2 11 12.5 13.8 15.2 16.5 18 19 19.6 19.8 20 20.4 20.6 21.7
28]*6.45e3  %Lines/sq.in
H=[0 0.18 0.26 0.38 1.4 1.8 3 5 9.5 28 70 160 260 370 420 520 825 1000 2000
8000]*2.021  %A-t/in
%Activate to plot B-H curve
%m=15; plot(H(1:m),B(1:m)); grid; pause;   %Linear plot
%xlabel ('Magnetizing Intensity (H), A-t/inch');
%ylabel ('Flux Density (B), kilolines/sq-in');
%title ('Magnetization Curve for M-22 ESS, 26 gage');
n=length(B); k=0;
if Bx==0; k=-1; y=0; end
if Bx<0; k=-1; y=0; disp('WARNING- Bx<0, Hm22=0 returned'); end
if Bx>B(n); y=H(n); k=-1; disp('CAUTION- Beyond B-H curve'); end
for i=1:n
if k==0 & (Bx-B(i))<=0; k=I; break; end
end
if k>0;
y=H(k-1)+(Bx-B(k-1))/(B(k)-B(k-1))*(H(k)-H(k-1));
else;
end
```

APPENDIX F

MATLAB Source Codes of Magnetization Curve for AISI 1010 Steel Frame

<H1010.m>   B-H interpolation routine

```
function y=y1010(Bx);
%Hx is AISI 1010 steel frame
%B-H values that follow are valid for 1010 steel plate
B=[0 2.6 5.2 7.7 10.3 12.9 18.1 24.5 31 38.7 51.6 64.5 71 77 83.8 90.3 97 103
110 116 122 129 135 142 150 260]*1000;
H=[0 0.6 1.3 2 2.5 2.8 3.4 4 4.7 5.5 6.9 8.5 9.9 11.9 14.3 19.2 28.3 46.5 86.9
155.6 242.5 444.6 647 950 2021 4e4];
%Activate values to plot B-H curve
%m=26; plot(H(1:m),B(1:m)); grid;pause; %Linear plot
%xlabel ('Magnetic Field Intensity (H), A-t/inch');
%ylabel ('Flux Density (B), kilolines/sq-in');
%title ('Magnetization Curve for AISI 1010 Steel Frame');
n=length(B); k=0;
if Bx==0; k=-1; y=0; end
if Bx<0; k=-1; y=0; disp('WARNING -Bx<0, Hx=0 returned'); end
if Bx>B(n); y=H(n); k=-1; disp('CAUTION - Beyond B-H curve'); end
for i=1:n
if k==0 & (Bx-B(i))<=0; k=i; break; end
end
if k>0;
y=H(k-1)+(Bx- B(k-1))/(B(k)- B(k-1))*(H(k)- H(k-1));
else;
end
```

APPENDIX G

MATLAB Source Codes of Magnetization Curve for DC Motor

<Magnetcurve.m>

```
clear;
info,
kE=1.666667e-10*p*N*2*nc/a;
kT=1.173e-9*p*N*2*nc/a;
phiR=TdR/kT/IaR;
%Plot magnetization curve for dc motor
%Build apparent tooth flux density array
Bt=linspace(0,100000,500); %generate N points(100) between 0 and 100000
for i=1:length(Bt); Ht(i)=hm22(Bt(i)); end
lam3=pi*(d-4/3*ds)/N;  %slot pitch calculated at one-third tooth depth from the
bottom
kt=3.2* (SF*lam3/ (lam3-bs)-1); %permeability of parallel air path
for i=1:length(Ht)
Ba(i)=Bt(i)+kt*interpl(Bt,Ht,Bt(i)); end
taut=fix(chi*N/p)+0.5;     %Teeth per pole span
At3=SF*la*(lam3-bs)*taut;    %Total tooth area @ 1/3 depth
dshft=4.0;            %Armature dimension
rc=(d-2*ds-dshft)/2;
Ac=2*SF*la*rc;          %Rotor core area
Af=wf*tf;             %Frame area
taup=taut*p/ N*pi/ 4*(d+2*delta);  %Pole arc
Ask=SF* (la+0.125)* wsk;      %Pole shank area
Ash3=SF* (la+0.125)* (2*wsk+taup)/3;   %Shoe area @ 1/3 depth
qty=lambda* (5*delta+bs);
ks=qty/ (qty-bs^2);       %Carter coefficient
phip=linspace(0,1.2*phiR,500); %generate flux per pole point within range 0 to
200
phip=[phip phiR];   m=length(phip);
for i=1:m
ATt=interpl (Ba,Ht,phip(i)/ At3)*ds;
ATc=hm22(phip(i)/ Ac)* pi/2/p* (d-ds-rc/2);
```

72

```
ATf=hx(LF* phip(i)/ Af/ 2)* pi/2/4*(Df-tf);
ATsh=hm22(LF* phip(i)/ Ash3)* lsh;
ATsk=hm22(LF* phip(i)/ Ask)*(Df-d-2*delta-2*lsh-2*tf)/2;
ATg=p*ks*delta*phip(i)/ pi/ 0.665/ d/ la/ 3.2;
ATp(i)=ATg+ATsk+ATsh+ATf+ATc+ATt;
end
plot(ATp(1:m-1), phip(1:m-1)/1000, ATp(m), phip(m)/1000, 'o');
title('Magnetization curve for dc machine'); grid;
xlabel('MMF per pole,A-t');
ylabel('Flux per pole, Kilolines');
```

APPENDIX H

MATLAB Source Codes of Performance Analysis for DC Shunt Motor

```
%Plot developed torque-speed curve for shunt excited dc motor with rated voltage
applied.
%Armature reaction neglected
clear; clf;
VtR=415;        %Rated terminal voltage(V)
PsR=400;        %Rated output horsepower(hp)
nmR=1800;       %Rated speed(rpm)
Ra=0.01271;%Armature resistance(Ohm)
eTaR=0.95;      %Efficiency
a=0.4; b=1.2e-5;   %F&W loss equation coefficients
%Rated developed torque(unit in ft.Lb). Assumption of 5% rotational losses.
TdR=5250*PsR/0.95/nmR
%Rated armature current (unit in Ampere)
IaR=746*PsR/eTaR/VtR;


load ('C:\MATLAB6\fyp\eif.txt');        %Load eif data
m=length(eif); npts=200;
KphiR=eif(1:m,1)/(nmR*pi/30); If=eif(1:m,2);
%Develop rated field current (If)
IfR=interp1(KphiR,If,(VtR-IaR*Ra)/(nmR*pi/30));
Rfeq=VtR/IfR;   %Total shunt field circuit resistance
npts=25; Ia=linspace(1.5*PsR*746/VtR, 0, npts);


%Plot torque versus speed (Td-nm)
for i=1:npts
    Kphi=interp1(If, KphiR, IfR);
    Td(i)=Kphi*Ia(i);
    wm(i)=VtR/Kphi-Td(i)*Ra/Kphi^2;
    nm(i)=wm(i)*30/pi;
    Pfw=a*nm(i)+b*nm(i)^2.7;
    eff(i)=(1-(Pfw+Ia(i)^2*Ra+VtR+IfR)/ (IfR+Ia(i))/VtR)*100;
    Ps(i)=(Td(i)*wm(i)-Pfw) / 746;
```

```
    if eff(i)<0; m=i-1; break; end  %F&W over driving
end


subplot(2,2,1);  plot(0,0,0.96*Td(1:m), nm(1:m), 0.96*TdR, nmR, 'r:o'); grid
title ('Shunt dc motor');
ylabel('Speed, rpm');  xlabel('Torque, ft-Lb');
subplot(2,2,2); plot(0,0,Ia(1:m)+IfR, nm(1:m), IaR+IfR, nmR, 'g:*'); grid
title ('Shunt dc motor');
ylabel('Speed, rpm');  xlabel('Line current, A');
subplot(2,2,3); plot(Ps(1:m), nm(1:m), PsR, nmR, 'b:o'); grid
title ('Shunt dc motor');
ylabel('Speed, rpm');  xlabel('Output power, hp');
subplot (2,2,4); plot(eff(1:m), nm(1:m), 95, nmR, 'c:*'); grid
title ('Shunt dc motor');
ylabel ('Speed, rpm'); xlabel('Efficiency, %')
```

APPENDIX I

Eif.txt – data input to be loaded into <Shunt.m>

5.0000000000000000e+000	0.0000000000000000e+000
3.3754945320409560e+001	5.0000000000000000e-002
6.2500000000000000e+001	1.0000000000000000e-001
9.1148160780059280e+001	1.5000000000000000e-001
1.1961242440187520e+002	2.0000000000000000e-001
1.4780578760673590e+002	2.5000000000000000e-001
1.7564124713592920e+002	3.0000000000000000e-001
2.0303179973074300e+002	3.5000000000000000e-001
2.2989044213246520e+002	4.0000000000000000e-001
2.5613017108238380e+002	4.5000000000000000e-001
2.8166398332178680e+002	5.0000000000000000e-001
3.0640487559196200e+002	5.5000000000000000e-001
3.3026584463419720e+002	6.0000000000000010e-001
3.5315988718978060e+002	6.5000000000000000e-001
3.7500000000000000e+002	7.0000000000000010e-001
3.9572523670681530e+002	7.5000000000000000e-001
4.1537887855487400e+002	8.0000000000000000e-001
4.3403026368949550e+002	8.5000000000000010e-001
4.5174873025599940e+002	9.0000000000000000e-001
4.6860361639970510e+002	9.5000000000000000e-001
4.8466426026593220e+002	1.0000000000000000e+000
5.0000000000000000e+002	1.0500000000000000e+000
5.1466839300048620e+002	1.1000000000000000e+000
5.2867987367899990e+002	1.1500000000000000e+000
5.4203309570040890e+002	1.2000000000000000e+000
5.5472671272958040e+002	1.2500000000000000e+000
5.6675937843138210e+002	1.3000000000000000e+000
5.7812974647068120e+002	1.3500000000000000e+000
5.8883647051234530e+002	1.4000000000000000e+000

5.9887820422124170e+002 1.4500000000000000e+000

6.0825360126223800e+002 1.5000000000000000e+000

6.1696131530020160e+002 1.5500000000000000e+000

6.2500000000000000e+002 1.6000000000000000e+000

6.3237409477997800e+002 1.6500000000000000e+000

6.3911118207239100e+002 1.7000000000000000e+000

6.4524463006297140e+002 1.7500000000000000e+000

6.5080780693745210e+002 1.8000000000000000e+000

6.5583408088156570e+002 1.8500000000000000e+000

6.6035682008104470e+002 1.9000000000000000e+000

6.6440939272162210e+002 1.9500000000000000e+000

6.6802516698903030e+002 2.0000000000000000e+000

6.7123751106900200e+002 2.0500000000000000e+000

6.7407979314727020e+002 2.1000000000000000e+000

6.7658538140956700e+002 2.1500000000000000e+000

6.7878764404162560e+002 2.2000000000000000e+000

6.8071994922917840e+002 2.2500000000000000e+000

6.8241566515795820e+002 2.3000000000000000e+000

6.8390816001369750e+002 2.3500000000000000e+000

6.8523080198212920e+002 2.4000000000000000e+000

6.8641695924898580e+002 2.4500000000000000e+000

6.8750000000000000e+002 2.5000000000000000e+000

6.8851329242090460e+002 2.5500000000000000e+000

6.8949020469743210e+002 2.6000000000000000e+000

6.9046410501531520e+002 2.6500000000000000e+000

6.9146836156028670e+002 2.7000000000000000e+000

6.9253634251807910e+002 2.7500000000000000e+000

6.9370141607442530e+002 2.8000000000000000e+000

6.9499695041505780e+002 2.8500000000000000e+000

6.9645631372570930e+002 2.9000000000000000e+000

6.9811287419211250e+002 2.9500000000000000e+000